

See discussions, stats, and author profiles for this publication at: <https://www.researchgate.net/publication/390548904>

# Phosphorite deposits: A promising unconventional resource for rare earth elements (REEs)

Article in *Geoscience Frontiers* · April 2025

DOI: 10.1016/j.gsf.2025.102044

---

CITATIONS

0

---

READS

84

6 authors, including:



**V. Balaram**

CSIR-National Geophysical Research Institute Hyderabad -500007

271 PUBLICATIONS 8,649 CITATIONS

[SEE PROFILE](#)

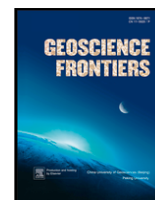


**Akhtar R. Mir**

University of Kashmir

28 PUBLICATIONS 264 CITATIONS

[SEE PROFILE](#)



## Review

# Phosphorite deposits: A promising unconventional resource for rare earth elements (REEs)

Shamim A. Dar<sup>a, \*</sup>, V. Balaram<sup>b</sup>, Parijat Roy<sup>c</sup>, Akhtar R. Mir<sup>d</sup>, Mohammad Javed<sup>a</sup>, M.Siva Teja<sup>e</sup>

<sup>a</sup> Department of Geology, Banaras Hindu University, Varanasi 221005 UP, India

<sup>b</sup> CSIR-National Geophysical Research Institute (NGRI), Hyderabad 500 007, India

<sup>c</sup> National Centre for Polar and Ocean Research, Ministry of Earth Sciences, Goa 403804, India

<sup>d</sup> Department of Earth Sciences, University of Kashmir, Srinagar 190006, India

<sup>e</sup> Department of Geology, Acharya Nagarjuna University, Guntur 522510, India

## ARTICLE INFO

## Article history:

Received 26 October 2024

Received in revised form 8 March 2025

Accepted 29 March 2025

Handling Editor: Federico Lucci

## Keywords:

Phosphorite deposits

Phosphate phases

REE

Bioleaching

Extraction

Recovery

## ABSTRACT

The green energy transition relies heavily on critical metals, such as Rare Earth Elements (REEs). However, their reserves are primarily focused in a few countries, such as China, which accounts for approximately 70 % of global production. Hence, several countries are currently looking for alternative resources for REE. Alternative REE resources in the supply chain include recycling of e-waste, industrial waste like red mud and phosphogypsum, coal ash, mine tailings, ocean floor sediments, and even certain types of sedimentary deposits like phosphorites where REE are present in lower concentrations but at larger volumes compared to primary ore deposits which are becoming targets by REE industry. Currently, several studies are going on the development of eco-friendly REE extraction technologies from phosphorite deposits. Consequently, advanced data analysis tools, such as Machine Learning (ML), are becoming increasingly important in mineral prospectivity and are rapidly gaining traction in the Earth sciences. Phosphorite deposits are mainly used to manufacture fertilizers as these rocks are known for their significant phosphorus content. Moreover, these formations are considered a prospective resource of REEs. The different types of phosphorite deposits such as continental, seamount, and ore deposits worldwide reported concentrations of  $\Sigma$ REE upto 18,000  $\mu\text{g/g}$ . Due to the augmented claim of REE for various ultra-modern, and green technology applications that are required to switch over to a carbon-neutral environment, these phosphorite deposits have become an important target mostly because of their relatively higher content of REE especially heavy REE (HREE). For example, Mississippian phosphorites reported  $\Sigma$ HREE 7,000  $\mu\text{g/g}$ . To have a comprehensive understanding of the REE potential of these phosphorite deposits which also include several Chinese phosphorite deposits, this study is undertaken to review the phosphorite deposits in the world and their REE potential, in addition to some of the associated aspects such as applications and formation mechanisms for different types of phosphorite deposits such as igneous phosphate deposits, sedimentary phosphorite deposits, marine phosphorite deposits, cave phosphate deposits, and insular guano deposits. Other important aspects include their occurrences, types, geochemical characteristics, the REE enrichment mechanisms, and various recovery methods adopted to recover REE from different phosphorite deposits. The present review paper concludes that the recent studies highlight the global potential of phosphorite deposits to satisfy the increasing demand for REEs. Extracting REE from phosphorite presents no significant technological or environmental difficulties, as long as radioactive elements are eliminated. In India, more comprehensive geological surveys, along with the advancement of new methods and evaluations, are required to locate phosphorite deposits with high concentrations of REEs.

© 20XX

## 1. Introduction

The lanthanide series of elements (La, Ce, Pr, Nd, Pm, Sm, Eu, Gd, Tb, Dy, Ho, Er, Tm, Yb, and Lu) along with Y and Sc are grouped and are called REE. Finnish chemist Johan Gadolin was the first person to discover rare earth elements (REEs) in 1794 while studying the mineral gadolinite. Further, in 1797 Swedish chemists called such elements as

yttria earths. Later in 1803, the concurrent discovery of REE was performed by M. Klaproth (German chemist) and J. Berzelius (Swedish chemist) in the mineral cerite. In 1814, Berzelius and Gan proposed the initial classification of these elements in two categories: the Y group and the Ce group. Currently, based on their atomic numbers and distinct physical and chemical properties, they are characterized into three

\* Corresponding author.

E-mail address: [sjshamim@bhu.ac.in](mailto:sjshamim@bhu.ac.in) (S.A. Dar).

<https://doi.org/10.1016/j.gsf.2025.102044>

1674-9871/© 20XX

sections (Brouziotis et al., 2022; Balaram, 2023a; Vadakkepuliambatta et al., 2024):

Light rare earth elements (LREE): La, Ce, Pr, Nd, and Pm.

Middle rare earth elements (MREE): Sm, Eu, Gd, Tb, Dy, and Ho.

Heavy rare earth elements (HREE): Er, Tm, Yb, and Lu.

The acronym 'REY' is often used when yttrium is added to  $\sum$ REE. REE in its metallic form is frequently established in nature; however, REE is normally present as compounds or isomorphisms within minerals (Di and Ding, 2024). REE has fascinated the consideration of numerous researchers due to its significant practical and scientific relevance. These metals have become extremely important worldwide for the required green energy transition to combat the current climate crisis through the extensive application of green technologies (Golroudbary et al., 2022; Balaram, 2023a; Balaram et al., 2024; Santosh et al., 2024). Particularly elements like Dy, Gd, Pr, and Sm are in great demand for industrial products such as magnets, wind turbines, solar panels, computers, and several other defense applications. In addition, REEs are basic components in several high-technology products such as lasers, guidance systems, electronic display systems, mobile phones, radar technology, and powerful electronic chips. REEs are utilized in metallurgy as alloys for various steel types (Bai et al., 2024). In nonferrous metallurgy, REE enhances the superiority of different alloys. The extraction of REE has significantly increased in recent years. An average of 4,500 tons of REE were mined worldwide from 1930 to 1939, but in 1955, the amount mined rose to 32,000 tons. Their applications have become highly varied (Gerasimovsky, 1959). Earlier simple combination of REE was performed in substantial amounts; however, due to increased industrial demand for some of them, the mining of individual elements has been performed in large amounts. Additionally, REE plays a crucial role in electrotechnology for preparing carbon electrodes in arc lamps and projectors to achieve the utmost light. In chemical manu-

facturing, they serve as catalysts in producing synthetic fabrics, plastics, and oil-cracking materials. In the light industry, they are used as dyes for leather and textiles, as well as in textile impregnation and weaving. In the silicate industry, REE contributes to producing glass that transmits infrared rays while absorbing ultraviolet rays, acting as coloring and decolorizing agents, and polishing optical glass. Moreover, they are vital tools for addressing geochemical challenges (Taylor et al., 1981).

REE deposits are distributed globally, but there is currently a shortage due to a decline in economically viable sources. The leading producers of REE ore include China, the United States, Myanmar, Australia, and Thailand. Notably, Myanmar has seen a surge in REE mining activity in 2023, as revealed by 30-meter resolution Landsat data (Chinkaka et al., 2023). Primary sources of REE are alkaline igneous rocks, carbonatites, pegmatites, veins, iron oxide copper-gold deposits, and skarn deposits (Wang et al., 2020; Balaram, 2022). Secondary deposits often result from the extensive alteration of igneous rocks, pegmatites, and iron oxide copper-gold deposits. Beach sands may contain minerals like monazite, rutile, ilmenite, zircon, garnet, and sillimanite, as well as ion-absorption clays, and weathered rocks rich in REEs. Some REE-bearing minerals like monazite and xenotime could accumulate with other heavy minerals along coastal areas (Sengupta and Van Gosen, 2016; Papadopoulos et al., 2019). Fig. 1 illustrates various types of REE resources, including promising alternative resources like phosphorite deposits. These economically viable deposits are limited to specific geological environments. Moreover, several unconventional REE resources such as phosphorites, coal and its burning by-products, oil sands tailings, and formation waters may help meet the rising demand for REE (Balaram, 2023a; Bishop and Robbins, 2024).

Phosphate ores are recognized for their varying concentrations of rare earth elements (REEs), which are often present in significant

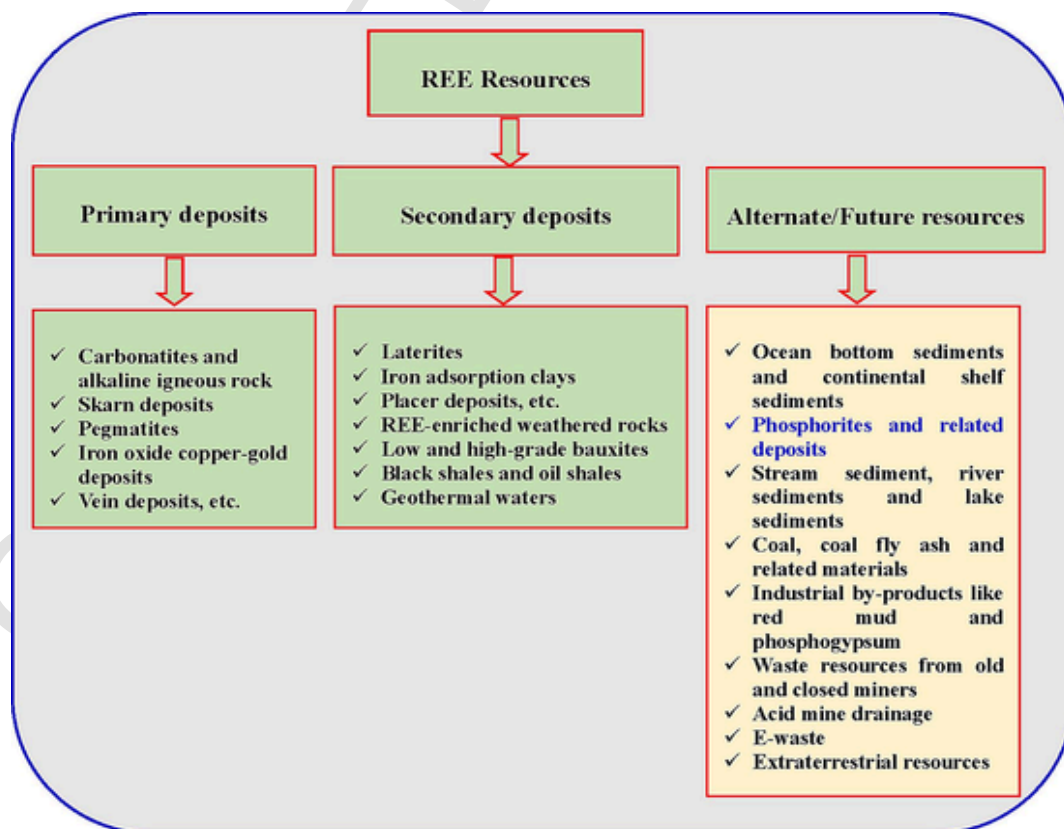


Fig. 1. Illustrative view of different types of Rare Earth Element (REE) resources, including the future potential alternative resources such as phosphorite deposits (modified after Balaram, 2023a,b).

amounts. The incorporation of REEs into phosphate-based products has the potential to promote enhanced growth and development in both plants and animals. Over the past few decades, global rare earth elements including (REE + Y) demand driven by the growing need for technological advancements, has experienced a substantial increase (Haxel et al., 2002; Van Gosen et al., 2014), resulting in an increase in rare-earth oxides production (U.S. Geological Survey, 2021). China dominates the global supply, meeting approximately 98 % of the demand, with a major contribution from an ion-exchange clay deposit in southern China, which serves as a primary source for medium and heavy rare earth elements (MREE and HREE) (Alonso et al., 2012). Rare earth elements (REE), recognized as significant minerals essential for fresh energy technologies, are experiencing a sharp rise in claims. However, significant deposits are found in limited geological settings like carbonatites and ion-adsorption clays, and unconventional secondary sources, including those from sedimentary basins, may hold the potential to address this growing claim. Phosphorites, coal and its burning by-products, oil sands tailings, and formation waters have all attracted attention for REE recovery, hitherto these sources stay largely under investigation. The global REE market is expanding quickly, motivated by increasing requirements and inadequate making, leading to greater attention in extracting REE from secondary sources like phosphate deposits.

The reduction of primary REE natural raw materials has forced to search for alternative resources such as phosphorite deposits. Because of significant concentrations of REE and Y in phosphate and phosphorite deposits, there has been increased interest, these deposits are progressively believed to stand as important sources of REE and have great demand currently because conventional deposits are unable to meet the demand for REE in the foreseeable future. For example, USGS found significant quantities of REE in phosphate nodules in Chatham Rise (east of New Zealand) which led to the setting up of an exploration company called Pacific Rare Earths Limited by Chatham Rock Phosphate Limited in 2018 (<https://www.nzx.com/announcements/404551>). In addition to their economic value, phosphorites are also useful in understanding several aspects such as major redox shifts, continental weathering rates, paleo-environmental conditions, and paleo-biochemical characteristics of the oceans (Föllmi, 1996). Because of all these developments, an endeavor is taken here to put forward a systematic study on the REE potential of phosphorite and phosphate rock deposits, or phosphate ores, and their distributions over a range of land and oceanic environments.

## 2. Phosphorites

Phosphorite is a phosphorus-rich, bioelemental sediment commonly linked to coastal upwelling. It can form in both terrigenous clastic and carbonate depositional environments, resulting in a variety of associated lithofacies. The phosphorus content in phosphorite typically exceeds 18 wt%  $P_2O_5$  (Blatt and Tracy, 1996; Daessle and Carriquiry, 2008), and can reach as high as 40 wt%, making it a key ore for fertilizers. Significant deposits have been discovered in the United States, North Africa, the Middle East, and China. The phosphorites of North Africa and the Middle East belong to the Late Cretaceous South Tethyan Phosphogenic Province (STPP), the biggest build-up of phosphorite on Earth. Beyond its economic importance, phosphorite plays a crucial role as the primary long-standing sink in the global phosphorus cycle. Phosphorus is an essential element in all living cells, playing key roles in various metabolic processes (Albaum, 1952). It is crucial for starch synthesis, a core component of nucleic acids, potentially necessary for photosynthesis, a major part of bones and teeth, and important for the shell formation process in many organisms. Within then necessary plant nutrients, phosphorus is comparatively limited in most soils, and its accessibility is a significant issue in regulating plant growth. Authigenic phosphate grains in sediments and rocks form concretions, including pellets, nodules, and crusts, predominantly made of the mineral franco-

lite ( $Ca_{10}(PO_4CO_3)F_{2-3}$ ). Fluorapatite is often present in cryptocrystalline forms, characterized by grain sizes smaller than 1  $\mu m$ , and is commonly known as “collophane” (Blatt and Tracy, 1996; Daessle and Carriquiry, 2008). These particles are typically embedded in a calcareous or siliceous matrix and can exhibit various colors, including green, brown, yellow, or white. Phosphorite beds can be a few centimeters to several meters thick and contain frequently approximately 30 %  $P_2O_5$ . The modifications of phosphorites make leaching of carbonates and sulfides and increase of  $P_2O_5$  content. The phosphorus (P) and phosphate ion ( $PO_4^{3-}$ ) participate as a primary role in living organisms and the sustainability of life on Earth (Godet and Föllmi, 2021). Natural phosphorites are important sources of phosphorous which accounts for about 0.1 % of the lithosphere (Shaban, 2016).

The most commonly recognized type of phosphate rock is sedimentary phosphate rock or phosphorite. Other varieties include phosphatized limestone, sandstone, shales, and igneous rocks. In comparison to other sediments of the ocean, phosphorite deposits are important REE resources, with  $\Sigma REE$  concentrations reaching up to 2000  $\mu g/g$ . Marine phosphorite deposits of all geological periods (from the Proterozoic to the recent) are found in seafloors. Phosphorite deposits are found all over the world in all continents except Antarctica (Fig. 2). Significant igneous phosphorite amounts are found in countries such as Brazil, Finland, Canada, South Africa, and Russia.

Phosphorites have been considered a significant economic ores used by humans since ancient times. Approximately world's 90 % of the total phosphate manufacture is employed in the production of various fertilizers which are crucial for agro-industries worldwide, as phosphorus is a vital nutrient essential for the growth and productivity of plants (Hellal et al., 2019). Although phosphorous is the 11th most abundant element (0.10 wt%) in the crust, it is a poor nutrient in some soil types (particularly calcareous soils) across the world. Because of the high organic stuff in the soil, the natural phosphate rock can dissolve very easily, when applied for nourishing agricultural productivity in Egypt (Hellal et al., 2019). Phosphorite/phosphate rock deposits are used for the industrial production of elemental phosphorous, and phosphoric acid which is used in making detergents, soaps, cleansers, and water softeners. Phosphates are added to common detergents to soften hard water to enhance the cleaning power of the detergent (Notholt, 1991; Zanin and Zamirailova, 2007; Dar, 2013; Dar et al., 2014). Elemental yellow phosphorus and phosphorus trichloride are used for the industrial production of glyphosate which is an extensively applied herbicide to kill some types of weeds and grasses.

### 2.1. Formation of phosphorite deposits

Phosphorite deposits are formed through two key processes: chemical and physical processes. A chemical process refers to the diagenetic discharge and concentration of phosphorus-retaining minerals, mainly in specific layers, influenced by various sedimentological and biogeochemical factors. Physical processes, on the other hand, engage the reworking and sedimentary capping of phosphorus-rich sediments. This process either concentrates comparatively heavy and insoluble phosphorus minerals or creates episodic changes in sedimentology that concentrate chemically mobilized phosphorus. Both processes can result from along-margin current dynamics or sea level fluctuations. Interestingly, phosphorus accumulation rates are highest (i.e., the phosphorus removal pump is most efficient) when phosphorites are not actively forming. Both physical and chemical processes are less common in deep-sea environments and rarely occur simultaneously in both space and time, even along continental margins. This rarity contributes to the limited availability of high-quality phosphorite deposits and phosphate rock reserves. This restriction is becoming increasingly crucial as a human claim for phosphorus greatly exceeds its geological replenishment, and few new phosphate rock prospects remain (Filippelli, 2011).



Fig. 2. A representative occurrence of phosphorite deposits in different parts of the world (modified after O'Brien and Heggie, 1988; Mazumdar et al., 1999; Ismail, 2002; Emsbo et al., 2015; Hein et al., 2016; Shaban, 2016; Cherepanov et al., 2019; He et al., 2022; Valetich et al., 2022; Graul et al., 2023; Yerkebulan et al., 2023).

Phosphorite also forms in oceanic upwelling regions, here huge quantity of phosphate-rich cold water rises from deep ocean layers to the surface. In warmer surface waters, the phosphate precipitates out of the solution and goes down to the seafloor, developing phosphorite deposits (Ritterbush, 1978). Originally, this deep ocean water was thought to rise to the shallow photic zone, where apatite precipitates directly from the ascending water column, accumulating as phosphate grains on the continental shelf (Cook and Shergold, 1984). Ahmed et al. (2022) found that the phosphorites in the Sirhan-Turayf area of north-western Saudi Arabia were formed from seawater other than detrital input, based on the reverse relationship between terrestrial components ( $\text{SiO}_2 + \text{Al}_2\text{O}_3 + \text{TiO}_2$ ) and authigenic components ( $\text{P}_2\text{O}_5 + \text{CaO} + \text{Na}_2\text{O}$ ), accompanied by very low levels of thorium. In China, Xiqiang et al. (2020) stated that the Zhijin phosphorites developed through the crystallization of apatite through the addition of REE and phosphorus-rich fluids with oxidizing seawater, facilitated by a local reducing environment that freed REY concentrations from ocean water. In the Sonrai region of the Paleoproterozoic Bijawar Basin in Uttar Pradesh, India, the phosphorites showed minimal diagenetic effects on the patterns of REE. Positive europium and negative cerium anomalies suggest a mixture of seawater and upwelling, with deposition occurring under fairly oxidizing to slightly reducing conditions (Khan et al., 2012a,b).

The Maghreb region, which includes the northern parts of Morocco, Algeria, Tunisia, and Libya, is home to some of the most significant and extensive phosphorite deposits in the world. These deposits, primarily composed of apatite minerals (a major source of phosphorus), have played a key role in global agriculture as a critical resource for fertilizer production. The formation mechanisms of the Maghrebian phosphorite deposits are complex and multifactorial, involving geological, oceanographic, and biological processes that occurred over millions of years. The primary phosphorite deposits in North Africa (Maghreb) formed during the late Cretaceous to early Cenozoic, with some of the most significant deposits dated to the Cenomanian-Turonian boundary (~93 million years ago). This period coincides with one of the most intense events of oceanic anoxia in the history of the Earth, which is believed to have provided favorable conditions for phosphorite deposition.

The formation of the phosphorites occurred over several phases, with the largest concentrations formed during times of global oceanic anoxia, particularly in the late Cretaceous. The stratigraphy of the phosphorite layers reveals that these deposits are typically found in the marine carbonates of the Tethys Ocean basin, intercalated with marls,

limestones, and clays. These phosphorites are linked to the tectonic evolution of the Tethys Sea, which existed between the African and Eurasian plates. Rifting and shallow marine conditions created ideal environments for phosphorite deposition in basins like those of Morocco and Tunisia. High primary productivity driven by oceanic upwelling in the region provided abundant phosphorus. This was particularly effective in shallow seas where nutrient-affluent deep waters were brought to the surface, stimulating phytoplankton growth. Hypoxic and anoxic circumstances in the bottom waters of these seas facilitated the preservation of organic material, increasing the concentration of phosphorus in the sediments. Phosphates, particularly in the form of apatite ( $\text{Ca}_5(\text{PO}_4)_3$ ), precipitated in sediments enriched by the decay of organic matter. The mineralization was aided by the high biological productivity of microorganisms like coccolithophores, which contributed to the phosphorus content. Phosphorite deposits in North Africa are a division of the Late Cretaceous-Eocene massive Phosphorite Belt, which stretches from the Caribbean to the Middle East. The deposits, having marine sedimentary origin, are thought to possess around 75 % of the phosphorite resources of the world.

According to the classification by Seredin (2010), the Northern African phosphorites, among the REE-bearing P-rocks, are considered to be promising to highly promising sources of REE, offering a precious and commercial substitute for critical REEs. Algerian and Tunisian phosphorites have high concentrations of  $\sum\text{REE}$  with negative Ce anomalies and significant LREE/HREE fractionations. In contrast, Moroccan phosphorites stand out due to their lower  $\sum\text{REE}$  levels, reduced (La/Yb)<sub>ch</sub> and (La/Gd)<sub>ch</sub> fractionations, and more distinct negative Ce anomalies. Interestingly, feeble differences in Eu anomalies were observed across the deposits, suggesting that the Eu/Eu\* ratio may serve as a provenance proxy, rather than a redox indicator, for these deposits.

Considering the paleogeographic context of phosphorite formation along the paleo-Tethys African margin, the chemical variations imply varying depositional circumstances. Specifically, the Ce/Ce\* values suggest that the basins of the Algeria–Tunisia system likely experienced sub-reducing to sub-oxic conditions, while those in Morocco were more sub-oxic to oxic, possibly reflecting differences in seawater supply (Buccione et al., 2021).

## 2.2. Classification of phosphate deposits

Phosphate deposits are classified into two types: igneous and sedimentary. Igneous ores are typically carbonatites (igneous rocks hold-

ing > 50 % by volume of carbonate minerals, Woolley and Kempe, 1989; Le Maitre, 2002). Sedimentary phosphate deposits, on the other hand, are a type of bioelemental sediment-chemical sedimentary rocks formed from the precipitation of nutrient elements such as phosphorus (P), iron (Fe), or silicon (Si) (Pufahl, 2010). Most sedimentary phosphatic ores are formed through upwelling, where deep, phosphorus-rich waters are brought to shallow shelves. Phytoplankton extract the phosphorus from the surface ocean and convert it into apatite, which accumulates in organic-rich mud below (Glenn et al., 1994; Jarvis et al., 1994). The dissolved phosphorus originates from the chemical weathering of continental rocks (Compton et al., 2000; Filippelli, 2008), linking both igneous and sedimentary phosphate deposits through the phosphorus cycle. Marine biochemical sedimentary rocks containing more than 18 wt%  $P_2O_5$  are classified as phosphorites (Glenn et al., 1994; Pufahl, 2010; Pufahl and Groat, 2016). About 80 % of phosphate ores originate from marine sources, about 17 % come from igneous rocks, while the rest deposits consist of residual sedimentary and guano-type sources (Broom-Fendley et al., 2021). Phosphate rock deposits of igneous and sedimentary origin are utilized in fertilizer manufacturing, containing up to 1 %  $\Sigma$ REE, making them potential future resources for REE. Seamount phosphorites contain REE higher than that of phosphorites of continental margin (Hein et al., 2016). The largest phosphate ore reserves of about 50 billion tons are found in Morocco (Fig. 3) then China holds 3.2 billion tons and Egypt holds 2.8 billion tons (Roshdy et al., 2023). According to the REE data in Table 1, phosphorite deposits globally show promise and may become a viable unconventional resource for REE in the future. Phosphate rock deposits have been reported to exist in different geological settings and intricate crystal structures (Abouzeid, 2008; Hellal et al., 2019; Di and Ding, 2024). Detailed description of these deposits is given in the following paragraphs:

### 2.2.1. Igneous phosphate deposits

The global distribution of igneous and sedimentary phosphorites is shown in Fig. 4a (Source: <https://firstphosphate.com/phosphate-industry/worldphosphatedeposits/>). Phosphatic ores are most commonly found in Phanerozoic carbonatites, although some silica-deficient alkalic intrusions can also contain high concentrations of apatite. Due to the wide variability in the morphology, composition, mineralogical associations, and tectonic settings of these igneous rocks, developing general exploration models is challenging. Typically, the phosphorus content in igneous phosphate rock ranges from 5 to 15 wt%  $P_2O_5$  (Table 2), but after mining, high-grade concentrates with minimal contaminants can be produced (Pufahl and Groat, 2016).

The Devonian Khibina Alkaline Complex of the Kola Peninsula of Russia, which includes seven deposits and four operating mines, is the biggest source of igneous phosphate in the world. In 2015, this complex produced 12.50 Mt, accounting for 58 % of global igneous phosphate rock production. In Brazil, igneous phosphate deposits, mostly linked to Cretaceous alkaline carbonatite complexes along the edges of Palaeozoic basins, produced 6.70 Mt, accounting for 31 % of global phosphate rock production in 2015. These deposits are generally associated with tectonic crustal flexuring or deep fault zones (Table 2; Jasinski, 2016; Pufahl and Groat, 2016). Although the Paleoproterozoic Phalabora Complex in South Africa only produced 2.20 Mt, accounting for 10 % in 2015, the country holds the biggest reserves of igneous phosphate rock, with 1,500 Mt, followed by Russia with 1,300 Mt and Brazil with 315 Mt (Table 2).

These deposits are extensive and have ages from Precambrian to Tertiary. Mineral phases of the apatite group preponderate in igneous and metamorphic rocks (Yerkebulan, et al., 2023). Igneous deposits gave nearly 10–20 % of world production in the last ten years. These deposits have been extracted in the Russian Federation, Kola Peninsula, Canada, South Africa, Brazil, Zimbabwe, and Finland. These are also reported to exist in Malawi, Uganda, Sri Lanka, and numerous other

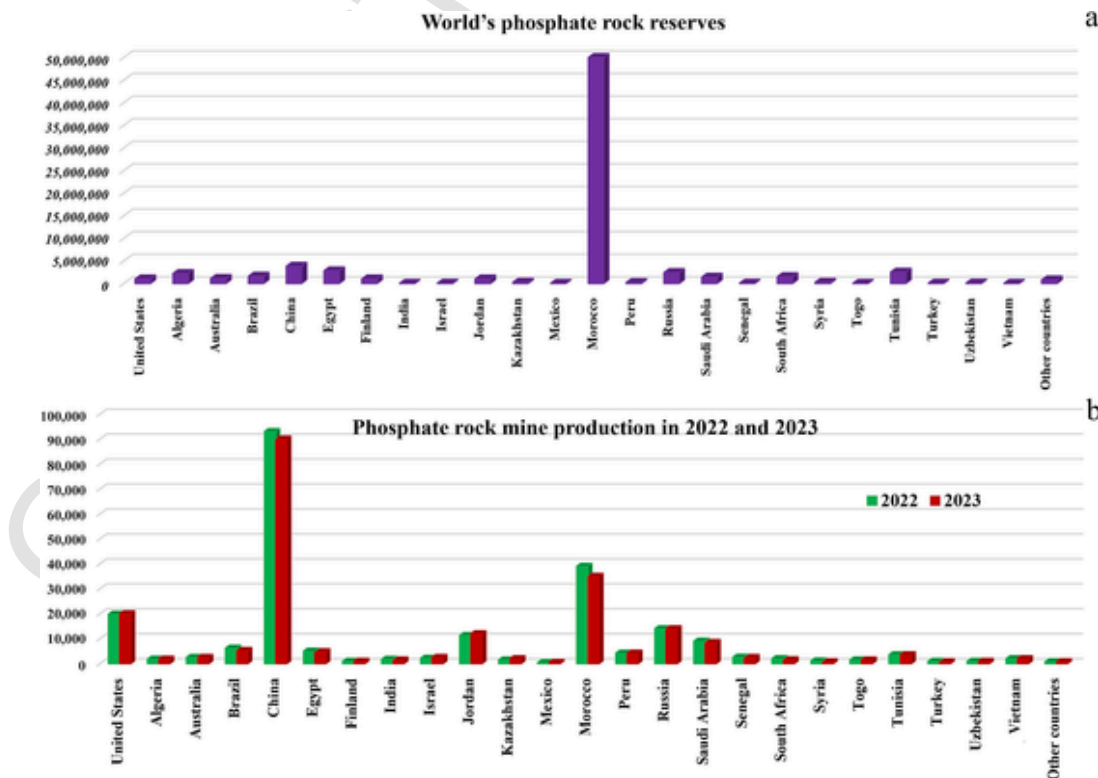


Fig. 3. (a) World's phosphate rock deposit reserves, (b) Phosphate rock mine production in 2022 and 2023. Reserves for China, India, Russia, and Turkey were revised based on Government reports. Reserves for South Africa were revised based on company reports (USGS, 2024).

**Table 1**

The concentrations of rare earth elements (REEs) in marine phosphorites and related rocks from different regions across the world.

| Ocean  | Phosphorites                    | Phosphorous content, wt %. | Average/range $\sum$ REE + Y or $\sum$ REE ( $\mu$ g/g) | Reference                |
|--|---------------------------------|----------------------------|---|--------------------------|
| Pacific and northeast Atlantic   | Seamount phosphorites           | 22.8 to 32.2               | 727   | Hein et al. 2016         |
|  | Continental margin phosphorites | 12.5 to 30.3               | 161   |                          |
| Doushantou Formation, South China  | Danzhai phosphorite deposit     | 21.1 to 25.7               | 21 to 447   | Yu et al. 2023           |
| Eastern Atlantic   | Seamount phosphorite deposits   | 33 %                       | –   | Jones et al. 2002        |
| Algerian Phosphorites  | Tébessa region                  | 13 to 28                   | 623   | Kechiched et al, 2020    |
| Ukrainian Phosphate Nodules  | Volyno-Podillya-Moldavia Basin  | 34.2                       | 1638 to 3602  | Sasmaz et al. 2023       |
| Phosphorites of Arkhara area of the Middle Amur region Far East Russia   | Continental margin phosphorites | 5 to 33                    | up to 813.58  | Cherepanov et al. 2019   |
| Meishucun excavation sites, South China                                  | Cambrian phosphorites           | 10 to 21.1                 | 99.1—709.7  | Shields and Stille, 2001 |
| Sedimentary Abu Tartur phosphate ore, Egypt                              | Phosphate ore                   | 30.1                       | 0.05–0.20 wt%   | Roshdy et al. 2023       |
| Mississippian phosphorites, US   | Phosphorite ore                 | –                          | 18,000 (7000 $\sum$ HREE)                               | Emsbo et al. 2015        |
| Phosphorites of the Georgina Basin of Australia                          | Phosphorite ore                 | 20.90 TO 36.30             | up to 0.5 wt% REE                                       | Valetich et al. 2022     |
| Chinese clay-type Phosphorite deposits                                   | Phosphorite ore                 | –                          | 500 to 2000   | Wu et al. 1996           |
| Hazm Al-Jalamis Phosphorites, Saudi Arabia                               | Phosphorites                    | 6.48 to 29.95              | <121.8  | Ahmed et al. 2022        |
| Pabdeh Formation, Khormuj anticline, SW of Iran                          | Phosphorites                    | 0.14 to 10.59              | 48 to 682   | Haddad et al. 2022       |
| Estonian   | Phosphorites                    | –                          | 600   | Graul et al. 2024        |
| Tébessa region, Eastern Algeria  | Phosphorites                    | 20.27 to 35.59             | 308 to 1029, avg. 621                                   | Ferhaoui et al. 2022     |
| Northern African phosphorite deposits (Morocco, Algeria and Tunisia)     | Phosphorites                    | 6.7 to 31.95               | 39.2 to 1759.4  | Buccione et al. 2021     |
| South China  | Phosphorus-bearing dolomites    | 1.88 to 9.66               | 330 $\sum$ REY  | Wu et al. 2022           |
|  | Phosphorus dolomites            | 10.3 to 18.1               | 676 $\sum$ REY  |                          |
|  | Phosphorites                    | 19.1 to 37.0               | 1477 $\sum$ REY   |                          |
| Bijawar Group, Sonrai Formation, Lalitpur district, Uttar Pradesh, India | Phosphorites                    | 28.78 to 31.84             | 2.89 to 236.91 $\sum$ REE                               | Dar, 2012                |

places (Habashi,1985). The comparison between igneous versus sedimentary phosphorite has been given in Table 2.

### 2.2.2. Sedimentary phosphorite deposits including marine phosphorite deposits

The world-known sedimentary phosphate deposits are shown in Fig. 4b (Pufahl and Groat, 2016). Sedimentary phosphate deposits are considered bioelemental sediments because they consist of precipitates of the nutrient element phosphorus (P) (Pufahl, 2010). Most sedimentary phosphate deposits contain over 18 wt% P<sub>2</sub>O<sub>5</sub>, with a maximum of around 35 wt%, and are therefore classified as phosphorites. These deposits are the prime source of phosphorus for fertilizer manufacture (Glenn et al., 1994; Pufahl and Groat, 2016).

The largest and most economically significant sedimentary deposits are found in North Africa, the Middle East, China, and the United States (Fig. 4b, Table 2 Pufahl and Grimm, 2003; Jasinski, 2016). The Doushantuo Formation in China, dating to the late Neoproterozoic, contains only 5 % of global phosphorus reserves but accounts for 45 % of global phosphorus production (Jasinski, 2016). In the United States, the middle Miocene Hawthorn Group in Florida and several corresponding Miocene deposits in North Carolina, USA contribute to 80 % of the country's phosphorus production, while the Permian Phosphoria Formation accounts for 10 %. These deposits are extensive, stratiform ore layers formed through a combination of biological, oceanographic, sedimentological, and diagenetic processes (Pufahl and Groat, 2016).

In comparison to igneous ores, the formation of sedimentary phosphate is closely tied to biological processes, with periods of global accumulation often reflecting significant changes in the biogeochemical cycling of phosphorus. One of the most important events in this regard was the Neoproterozoic Oxygenation Event (Och and Shields-Zhou, 2012; She et al., 2013), which not only paved the way for the evolution of multicellular animals but also led to the formation of the first large phosphorite deposits (Nelson et al., 2010; Pufahl and Hiatt, 2012; Drummond et al., 2015). As a result, sedimentary phosphates are primarily a Phanerozoic phenomenon, reflecting the impact of an evolving and expanding biosphere on phosphorus fixation (Pufahl and Groat, 2016).

Sedimentary phosphorite deposits are the predominant source of phosphate rock worldwide, found on all continents and accounting for about 95 % of global phosphate reserves (Howard, 1979). Most of the commercial deposits have a Phanerozoic age. The phosphorites are composed of crypto-crystalline carbonate fluorapatite that occurs as beds with thicknesses ranging from a few centimeters to several meters. Estonian phosphorites of the Baltic paleo basin are one of the largest phosphate rock reserves in Europe (Graul et al., 2024).

Phosphorites along with cobalt crusts and ferromanganese deposits are significant marine mineral deposits especially for REE (Gonzalez et al., 2016; Balaram, 2023b). Fig. 5 depicts the occurrence of phosphorites and other sedimentary deposits such as ferromanganese crusts, manganese nodules, massive sulfide deposits, REE-rich marine mud at the ocean basins, mid-oceanic ridges, seamounts, and continental margins in the oceans with the information on various critical metals in the respective deep-sea sediments and phosphorites (Balaram, 2023b). Marine phosphorites are classified as non-granular and granular phosphorites (Föllmi, 1996); these phosphorites provide vast knowledge regarding depositional and diagenetic variations (e.g., Föllmi, 1996). Continental weathering of pre-existing rocks and soils is the main source of phosphorus and subsequently, it is transferred in the form of dissolved, particulate, organic, and inorganic forms by rivers into the oceans (Godet and Föllmi, 2021). Marine phosphate deposits with authigenic apatite (main phase) exist widely along the continental margins of different continents. Continental margins are hosts for the mixture of continentally derived siliciclastic and marine and biogenic material (März et al., 2018). Phosphorus is absorbed by plants and animals and released back into seawater. In warm surface water bodies precipi-

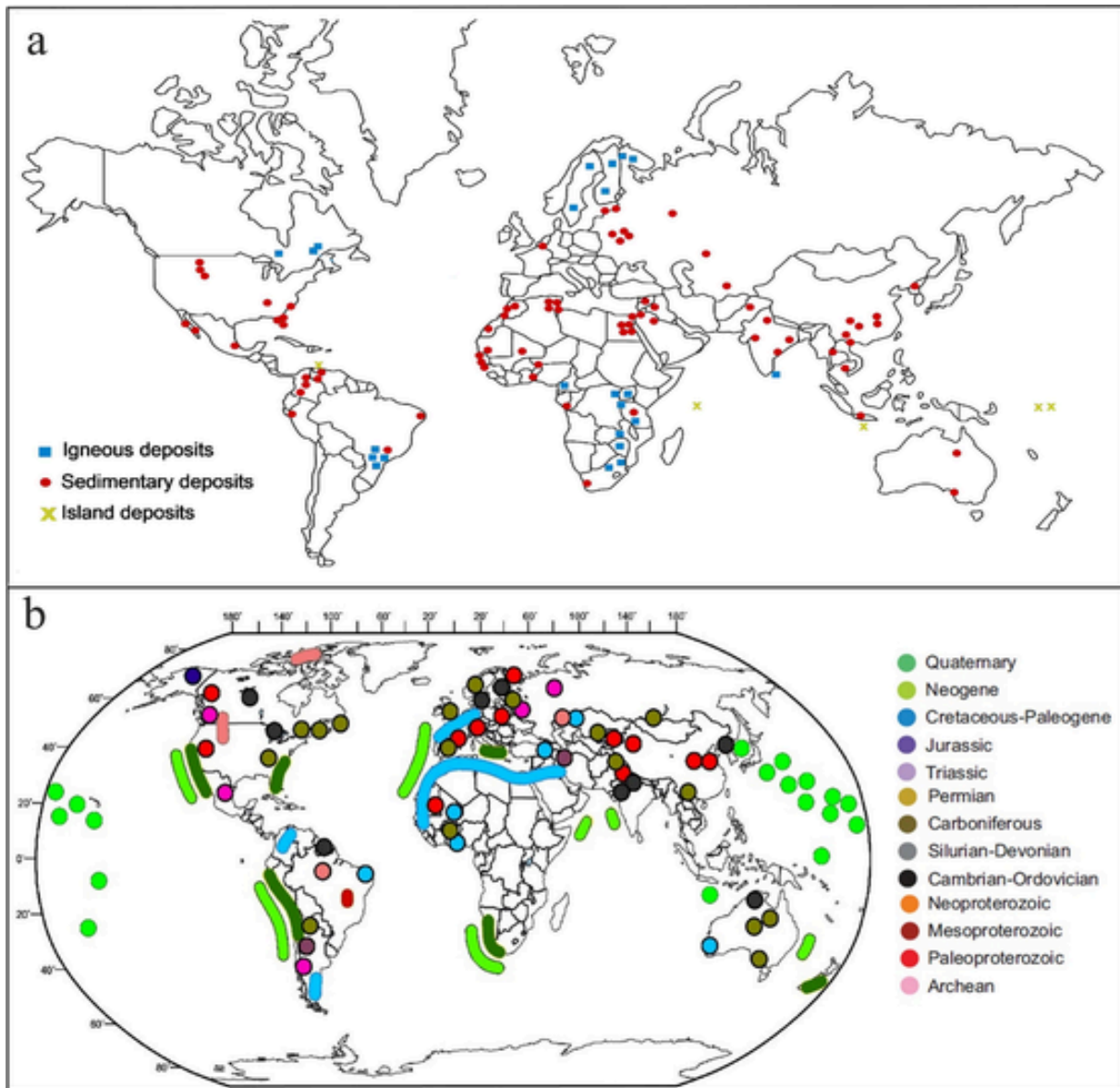


**Fig. 4.** (a) A known world's phosphate deposits., (b) Global distribution and ages of known sedimentary phosphorites (modified after). Source: Food and Agriculture Organization of the United Nations ([https://firstphosphate.com/phosphate-industry/worldphosphatedeposits/Pufahl and Groat, 2016](https://firstphosphate.com/phosphate-industry/worldphosphatedeposits/Pufahl%20and%20Groat,2016))

tation of phosphate occurs then such precipitates go down to the seafloor where they accumulate and form phosphorite deposits. In several cases, concentrations of phosphorus and REE in phosphorites formed on the surface of the slope of seamount volcanoes are positively correlated with the organic carbon content, which supports their coprecipitation from seawater enriched in REE supplied by hydrothermal vents (Cherepanov et al., 2019). Marine seamount phosphorites were found to contain a high  $\sum$ REE content with an average of 727  $\mu\text{g/g}$ , and a maximum content of 1992  $\mu\text{g/g}$ , with high HREE (He et al., 2022). Hein et al. (2016) reported 4–6 times higher individual REY contents and suggested that seamount phosphorites exhibit significantly higher concentrations of HREE compared to continental margin phosphorites. The higher concentrations of REE in seamount phosphorites may be due to various factors such as age. REE concentrations in seawater can vary over time due to factors such as variation in pH, water depth during creation, the presence of complexing ligands, and the organic carbon content during the deposition process.

### 2.2.3. Metamorphic deposits

Phosphorus concentrations in metamorphic rocks typically range from 0.01 % to 1.3 %. However, the available data on phosphorus in metamorphic rocks is limited compared to that of igneous rocks. In most instances, phosphorus tends to be comparatively immobile through metamorphism, meaning that the phosphorus content in metamorphic rocks generally reflects that of their unmetamorphosed precursors. Elliott (1973) studied the transition from gabbro to amphibolite and found that amphibolites had slightly higher  $\text{P}_2\text{O}_5$  contents than their unmetamorphosed counterparts (0.169 % versus 0.146 %, respectively). Koritnig (1978) suggested that phosphorus content generally increases with metamorphic grade, but the data on this are limited, and no comprehensive study has been conducted.

Metamorphic phosphate deposits are formed when existing phosphate deposits are transformed by metamorphism at high pressure and temperature. They are less common than sedimentary and igneous phosphate deposits. Metamorphic rocks have phosphorus concentra-

**Table 2**  
The World Phosphate Production and Reserves.

| Country                         | Mine production |               |               |
|---------------------------------|-----------------|---------------|---------------|
|                                 | 2014 (Mt)       | 2015 (Mt)     | Reserves (Mt) |
| <b>Igneous Phosphorites</b>     |                 |               |               |
| Brazil                          | 6.04            | 6.70          | 315           |
| Russia                          | 11.00           | 12.50         | 1,300         |
| South Africa                    | 2.16            | 2.20          | 1,500         |
| Total                           | 19.20           | 21.40         | 3,115         |
| % of world                      | 8.80            | 9.59          | 4.53          |
| <b>Sedimentary phosphorites</b> |                 |               |               |
| Algeria                         | 1.50            | 1.20          | 2,200         |
| Australia                       | 2.60            | 2.60          | 1,030         |
| China                           | 100.00          | 100.00        | 3,700         |
| Egypt                           | 5.50            | 5.50          | 1,250         |
| India                           | 1.11            | 1.10          | 65            |
| Iraq                            | 0.20            | 0.20          | 430           |
| Israel                          | 3.36            | 3.30          | 130           |
| Jordan                          | 7.14            | 7.50          | 1,300         |
| Kazakhstan                      | 1.60            | 1.60          | 260           |
| Mexico                          | 1.70            | 1.70          | 30            |
| Morocco/W. Sahara               | 30.00           | 30.00         | 50,000        |
| Peru                            | 3.80            | 4.00          | 820           |
| Saudi Arabia                    | 3.00            | 3.30          | 956           |
| Senegal                         | 0.90            | 1.00          | 50            |
| Syria                           | 1.23            | 0.75          | 1,800         |
| Togo                            | 1.20            | 1.00          | 30            |
| Tunisia                         | 3.78            | 4.00          | 100           |
| United States                   | 25.30           | 27.60         | 1,100         |
| Vietnam                         | 2.70            | 2.70          | 30            |
| Other countries <sup>a</sup>    | 2.37            | 2.60          | 380           |
| <b>Total</b>                    | <b>198.99</b>   | <b>201.65</b> | <b>65,661</b> |
| % of world production           | 91.20           | 90.41         | 95.47         |
| World total, all sources        | 2018.19         | 223.05        | 68,776        |

Finland estimated 2012 production = ca. 0.87 Mt, with current production from Siilinjärvi = ca. 11 Mt/yr with an average grade of 4 wt% P<sub>2</sub>O<sub>5</sub> and ore reserves of 234 Mt.

<sup>a</sup> Includes Chile, Colombia, Finland, Indonesia, Iran, North Korea, Pakistan, Philippines, Sri Lanka, Tanzania, Thailand, Uzbekistan, Venezuela, and Zimbabwe (modified after O'Brien et al., 2015; Jasinski, 2016; Pufahl and Groat, 2016).

tions varying from 0.01 % to 1.3 % (Nash, 1984). REE-hosting minerals like monazite, apatite, and xenotime, are commonly present in metamorphic phosphate rocks.

#### 2.2.4. Biogenic deposits

The initial theory, known as the “biological source” hypothesis, suggests that phosphorite forms through the build-up of biological remains (Tan et al., 2022; Yuan et al., 2016). Key terrestrial contributions to marine phosphorus include wind transmission and underground runoff (Lei et al., 2000). In contrast, the phosphorus input from submarine hydrothermal solutions and volcanic activity is insignificant (Warren, 2010).

The development of phosphate fossil formation is referred as phosphatization which needs the presence and accumulation of active phosphorus in an anoxic environment (Briggs & Kear, 1993). Another significant theory regarding phosphorite genesis is the “biological phosphorus formation” model. Modern marine research indicates that phosphorus cannot be directly precipitated from seawater in an inorganic form; instead, it relies on the complex life processes of organisms to absorb and incorporate disseminated phosphorus from the water (Yang et al., 2020). After these organisms die and are buried, they can undergo phosphatization. This method of fossil preservation is one of the main ways wherein fossils are specifically buried in the geological record.

The development of marine phosphates is a composite process which occurs in various settings, making it essential to have reliable proxies to reconstruct the conditions under which they formed. Phos-

phates serve as precious tracers of alterations in the marine phosphorus cycle, which are linked to disruptions in the global carbon cycle, especially during extensive carbon isotope excursions (Föllmi, 1996; Slomp et al., 1996; Filippelli, 1997; Filippelli, 2011; Delaney, 1998; Schenau et al., 2000; van der Zee et al., 2002; Slomp and Van Cappellen, 2007; Paytan and McLaughlin, 2007; Auer et al., 2016).

REEs are widely recognized as tracers of geochemical processes and are preferentially included into phosphates. This makes them valuable tools for reconstructing the paleoenvironmental circumstances that prevailed throughout the construction of marine authigenic and biogenic phosphates (Grandjean and Albarede, 1989; Grandjean-Lecuyer et al., 1993; Reynard et al., 1999; Morad and Felitsyn, 2001; Felitsyn and Morad, 2002; Lecuyer et al., 2004; Garnit et al., 2012). The examination of definite REE patterns, especially when evaluated to normalization standards like the Post-Archean Australian Shale (PAAS) standard, has been suggested as an effective method for characterizing the depositional environment and diagenetic overprints of marine phosphates (Shields and Stille, 2001; Haley et al., 2004; Garnit et al., 2012).

Marine carbonates and authigenic phosphates, which form through microbially mediated processes (such as Francolite), firstly integrate REE signatures from the seawater or pore water in which they precipitated (Elderfield and Pagett, 1986; Wright et al., 1987; Sholkovitz et al., 1994; Reynard et al., 1999; Shields and Stille, 2001; Lecuyer et al., 2004; Kalvoda et al., 2009). REEs can be included in the crystal structure by substituting calcium or through adsorptive uptake on the crystal lattice. Modern indications from marine sediment cores proposed that different REE patterns emerge under varying redox environments within the sediment. These patterns help to distinguish between REE signatures derived from particulate organic matter and those derived from iron oxide (German and Elderfield, 1990; German et al., 1991; Slomp et al., 1996; Haley et al., 2004; Garnit et al., 2012; Emsbo et al., 2015).

In contrast, biogenic phosphates typically do not include important amounts of REEs during their formation and have REE patterns similar to that of primary marine REE patterns in a pristine state (Elderfield and Pagett, 1986; Reynard et al., 1999). However, a few researchers have depicted that adsorption and substitution processes can result in major REE enrichment (Holser, 1997; Reynard et al., 1999; Shields and Stille, 2001). These processes are well documented in fossil mammal bones (Herwartz et al., 2011). Research on the effects of early and late diagenetic REE adsorption and substitution has demonstrated that these processes can completely mask the primary REE signal (Holser, 1997; Reynard et al., 1999; Shields and Stille, 2001). The fact that REE patterns can be altered by post-depositional diagenetic exchange (Elderfield and Pagett, 1986; German and Elderfield, 1990; Reynard et al., 1999) or surface weathering (McArthur and Walsh, 1984; Bonnot-Courtois and Flicoteaux, 1989) raises concerns about the reliability of REE patterns as paleoecological and paleoenvironmental tracers. Despite this evidence of post-formation alteration, shale-normalized REE concentrations in microbially mediated authigenic and biogenic phosphates are still commonly used as proxies to reconstruct paleoceanographic and paleoecological conditions during their formation or growth (Grandjean and Albarede, 1989; Grandjean-Lecuyer et al., 1993; Reynard et al., 1999; Lecuyer et al., 2004; Kalvoda et al., 2009). Cave phosphate deposits form a minor component having raw materials of only some thousand tons of phosphorite. The build-up of bird dropping forms insular guano deposits. The insular guano deposits make up only approximately 2 % of phosphate rock creation in the world. These are found in Peru, Chile, Mexico, Seychelles, the Arabian Gulf, the Philippines, and elsewhere and are categorized as low-island and high-island deposits (Cook and Shergold, 1984).

#### 2.2.5. Phosphate deposits as a result of weathering

Phosphorus is delivered to the ocean through the weathering of continental rocks in two states dissolved and particulate (Benitez-Nelson,

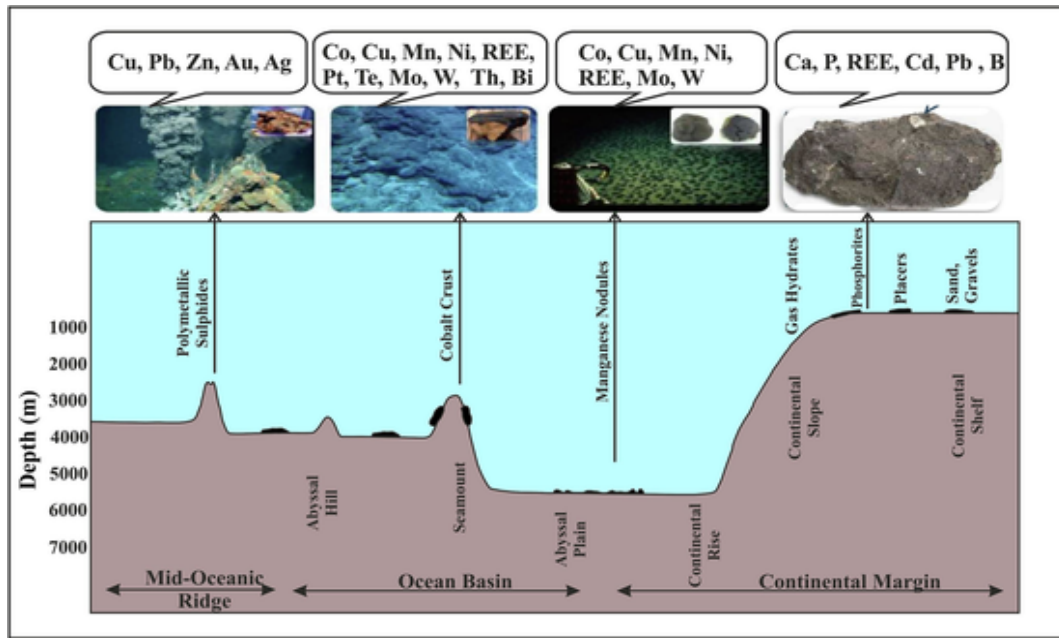


Fig. 5. Occurrence of phosphorites and other sedimentary deposits such as manganese nodules, ferromanganese crusts, massive sulfide deposits, REE-rich marine mud at the ocean basins, mid-oceanic ridges, seamounts, and continental margins in the oceans with the information on various critical metals in the respective deep-sea sediments (Balaram, 2023a,b).

2000; Filippelli, 2008, 2011). While river transport is the dominant pathway for phosphorus input, eolian dust, which supplies phosphorus adsorbed on particles, plays an important role, especially in arid climates (Drummond et al., 2015). Dissolved phosphorus exists as phosphate species ( $\text{H}_2\text{PO}_4^-$ ,  $\text{HPO}_4^{2-}$ ,  $\text{PO}_4^{3-}$ ), which are readily available for biological uptake. Most particulate phosphorus consists of insoluble phosphatic minerals from igneous and metamorphic rocks, which do not participate in the biogenic phosphorus cycle as they are not bioavailable. However, particulate forms with bioavailable phosphorus include detrital organic matter, clay minerals, and Fe-(oxyhydr) oxide particles that adsorb phosphorus (Filippelli, 2008). Microbial respiration of detrital organic matter releases phosphorus, converting it into phosphate. Phosphorus adsorbed onto clays and Fe-(oxyhydr) oxides is released through the high ionic strength of seawater and burial in reduced pore waters (Heggie et al., 1990; Mills et al., 2004; Drummond et al., 2015). Windblown clays and Fe-(oxyhydr) oxide particles are the primary source of eolian phosphorus.

Once in the marine system, dissolved phosphorus triggers biological productivity (Filippelli, 2008, 2011; Pufahl, 2010). In surface waters, away from the influence of rivers or coastal upwelling, phosphate concentrations are reduced to near zero due to phytoplankton fixation during photosynthesis, limiting sustained growth. Phosphate levels increase in deeper, older waters because organic matter cascading from surface layers is recycled, releasing phosphorus back into the seawater (Benitez-Nelson, 2000; Filippelli, 2008, 2011). This pattern of surface depletion and deep enrichment is typical of all nutrient elements in marine systems. These deposits are produced because of the weathering of all aforesaid deposits as the weathering of rocks causes the removal of phosphate ions (Flicoteaux and Lucas, 1984).

### 2.3. Mineralogy

There are more than 170 minerals that contain  $\geq 1\%$   $\text{P}_2\text{O}_5$ , however apatite accounts for over 95% of all phosphorus in the crust of Earth (Palache et al, 1951; Altschuler et al, 1958; Deer et al, 1962; Ptáček, 2016). Its structure allows for the substitution of various ele-

ments (Jarvis et al., 1994; Jiang et al., 2020; Pufahl and Groat, 2016, Table 3), such as small amounts of  $\text{VO}_4^{3-}$ ,  $\text{As}_2\text{O}_4$ ,  $\text{SO}_4^{2-}$ , and  $\text{CO}_3^{2-}$  can replace equivalent amounts of  $\text{PO}_4^{3-}$ . Fluoride ( $\text{F}^-$ ) can also partially or completely substitute for  $\text{Cl}^-$  or  $\text{OH}^-$ , with small traces of Mg, Pb, Sr, Mn, Li, Ce, Na, Y, and other REE compensating through ionic replacements. Consequently, a wide variety of apatite exists in nature, and different varieties may be found in the same locality (e.g. 'chloro-apatite' ( $\text{Ca}_{10}\text{Cl}_{12}(\text{PO}_4)_6$ ), 'fluor-apatite' ( $\text{Ca}_{10}\text{F}_2(\text{PO}_4)_6$ ), 'carbonate-apatite' ( $\text{Ca}_5(\text{PO}_4)_3(\text{CO}_3)(\text{OH},\text{F})$ ), 'hydroxyl-apatite' ( $\text{Ca}_{10}(\text{OH})_2(\text{PO}_4)_6$ ), 'oxy-apatite' ( $\text{Ca}_{10}(\text{PO}_4)_6\text{O}$ ) (Parker, 1971). A few main REE phosphate phases are given in Table 4.

Historically, it was believed that calcium phosphates in sedimentary series were primarily composed of a fluorine-retaining amorphous substance called "collophane" or "collophanite." Nevertheless, modern mineralogy suggests this amorphous material is a cryptocrystalline or microcrystalline substance and belong to the apatite group of minerals. The most common mineral found in sedimentary apatite's is carbonate fluorapatite (CFA) or francolite. As per Young (1975) and Slansky (1986), fluorapatite forms a hexagonal crystal structure. An average phosphorite composition includes about 80% apatite, 10% quartz, 5% muscovite-illite, 2% organic matter, and 1% dolomite-calcite. Common phosphate-bearing rocks include limestones and mudstones. Fig. 6a illustrates an X-ray diffraction spectrometer (XRD) pattern of raw phosphate, showing the presence of these major minerals.

During phosphate mining, the ore is purified and concentrated to obtain phosphate rock, and in this process, phosphatic clay and sand

Table 3

Some possible substitution in the apatite structure.

| Constituent ion    | Substituting ion   |
|--------------------|--|
| $\text{Ca}^{2+}$   | $\text{Na}^+$ , $\text{K}^+$ , $\text{Ag}^+$ , $\text{Sr}^{2+}$ , $\text{Mn}^{2+}$ , $\text{Mg}^{2+}$ , $\text{Zn}^{2+}$ , $\text{Cd}^{2+}$ , $\text{Ba}^{2+}$ , $\text{Sc}^{3+}$ , $\text{Y}^{3+}$ , $\text{REE}^{3+}$ , $\text{Bi}^{3+}$ , $\text{U}^{4+}$ |
| $\text{PO}_4^{3-}$ | $\text{CO}_3^{2-}$ , $\text{SO}_4^{2-}$ , $\text{CrO}_4^{2-}$ , $\text{AsO}_4^{2-}$ , $\text{VO}_4^{3-}$ , $\text{CO}_3$ , $\text{F}^-$ , $\text{CO}_3$ , $\text{OH}^{2-}$ , $\text{SiO}_4^{4-}$   |
| $\text{F}^-$       | $\text{OH}^-$ , $\text{Cl}^-$ , $\text{Br}^-$ , $\text{O}^{2-}$  |

(modified after Nathan, 1984; Jarvis et al., 1994; Shaban, 2016).

**Table 4**  
List of some important rare earth element (REE) phosphate minerals.

| Name of the mineral      | Chemical composition   |
|--------------------------|--|
| Apatite                  | $\text{Ca}_5(\text{PO}_4)_3(\text{OH}, \text{F}, \text{Cl})$   |
| Francolite               | $(\text{Ca}, \text{Mg}, \text{Sr}, \text{Na})_{10}(\text{PO}_4, \text{SO}_4, \text{CO}_3)_6\text{F}_{2-3}$ |
| Florencite               | $(\text{REE})\text{Al}_3(\text{PO}_4)_2(\text{OH})_6$  |
| Crandallite              | $\text{CaAl}_3(\text{PO}_4)_2(\text{OH})_6$  |
| Gorceixite               | $(\text{BaAl}_3)(\text{PO}_4)_2(\text{OH})_6$  |
| Fluorapatite             | $\text{Ca}_5(\text{PO}_4)_3\text{F}$   |
| Hydroxyapatite           | $\text{Ca}_5(\text{PO}_4)_3\text{OH}$  |
| Carbonate-hydroxyapatite | $\text{Ca}_{10}(\text{PO}_4)_{6-x}(\text{CO}_3)_x(\text{OH})_{2-x-2y}(\text{CO}_3)_y$                      |
| Monazite                 | $(\text{Ce}, \text{La}, \text{Nd}, \text{Th})\text{PO}_4 \cdot \text{SiO}_4$                               |
| Xenotime                 | $\text{YPO}_4$   |
| Phosphogypsum            | $\text{CaSO}_4 \cdot 2\text{H}_2\text{O}$  |

(modified after Rasmussen, 1996; Benataya et al., 2020; Hoshino, 2020).

are leftover. Then phosphate in the form of phosphoric acid is extracted from the phosphate rock. The residual phosphogypsum ( $\text{CaSO}_4$ ) also contains significant concentrations of REE (Rychkov et al., 2018; Laurino et al., 2019). Some of the important REE and REE-carrying minerals in phosphorites are shown in Table 4. The infrared spectrum of natural phosphate depicting various functional groups such as hydroxyl, carbonate, and phosphate which correlates with its mineralogy is presented in Fig. 6b.

### 3. Formation of phosphorite deposits through geological time

The age and worldwide distribution of sedimentary phosphorites is given in Fig. 4b. These deposits occur over a large geological time ranging from the Cambrian to the Pleistocene. These deposits have diverse chemical compositions and physical forms; mostly occur as relatively flat-lying thick beds. In Algeria, rich Palaeocene-Eocene phosphorites are found (Laouar et al., 2024). Further, REE-rich sedimentary phosphorites of the Paleocene-Eocene period occur in the mid-east and northern African countries (Buccione et al., 2021). The Precambrian-

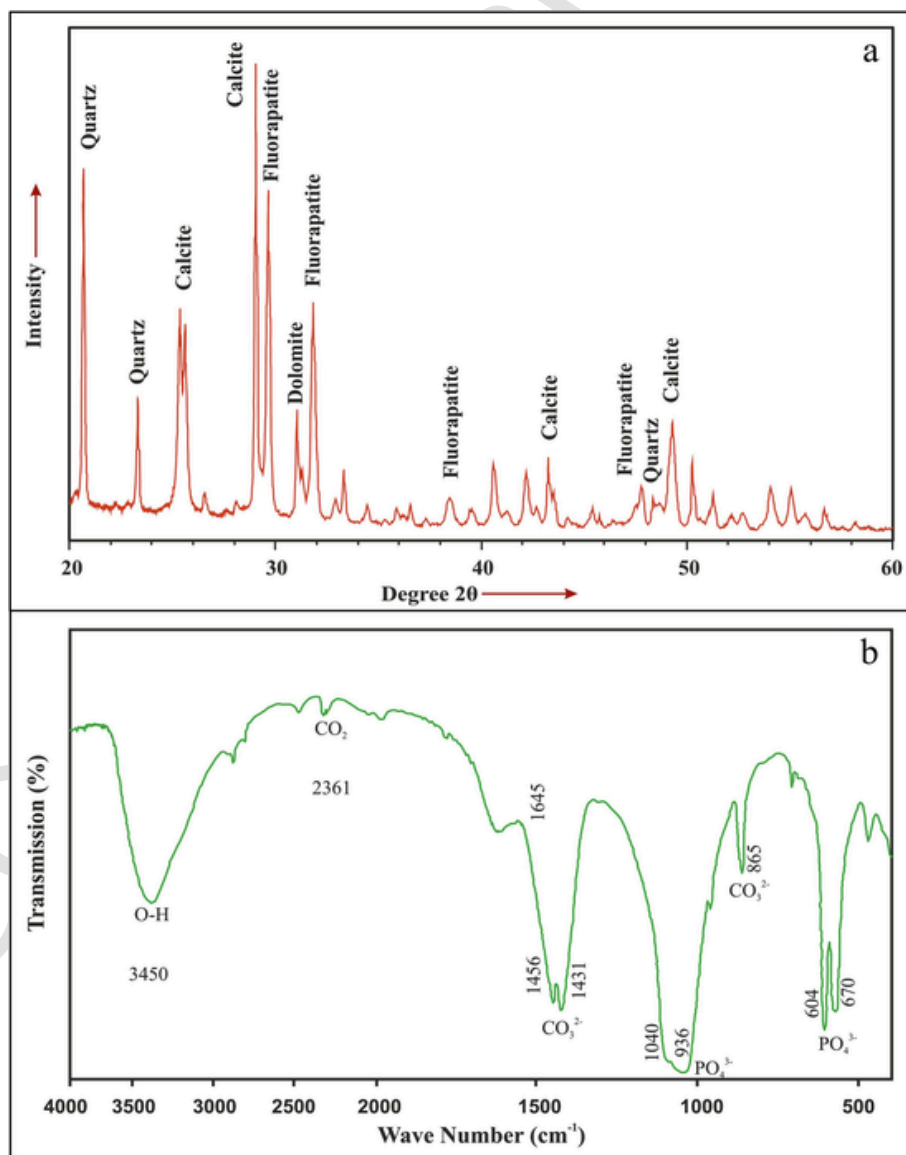


**Fig. 6.** (a) X-ray diffraction pattern of the raw phosphate (modified after Amine et al., 2019), (b) The infrared spectrum of natural phosphate depicts various functional groups such as hydroxyl, carbonate, and phosphate (modified after Maallah and Chtaini, 2018).

Cambrian boundary, around 540 million years ago, known as the ‘‘Cam-

**Table 5**  
The total rare earth elements ( $\Sigma$ REEs) and phosphate contents of phosphorites of different ages.

| Country   | Age                           | Age in My/Ma         | % P <sub>2</sub> O <sub>5</sub> | $\Sigma$ REE ppm              |
|---|-------------------------------|----------------------|---------------------------------|-------------------------------|
| Peru-Chili (off shore)                          | Holocene                      | 11.700 Yr to Present | 22.61                           | –                             |
| Florida (‘‘pebble’’)                            | Pliocene                      | 5.3 to 2.58 Ma       | 32.07                           | –                             |
| Venezuela (Riecito)                             | Miocene                       | 24 to 5 my           | 34.28                           | –                             |
| Algerian phosphorites                           | Paleocene-Eocene              | 66–33.9 my           | 19.65 to 21.32                  | 764 to 2050                   |
| Benin Mid.                                      | Eocene                        | 56 to 33.9 Ma        | 28.15                           | –                             |
| Morocco (Khouribga)                             | Early Eocene                  | 56 to 47.8 Ma        | 34.26                           | –                             |
| Tunisia (Metlaoui)                              | Early Eocene                  | 56 to 47.8 Ma        | 24.87 to 28.30                  | 283 to 549                    |
| Egypt (Quseir)                                  | Late Cretaceous               | 100.5 to 66 my       | 25.8 to 29.8 %                  | 343.8 to 640.8                |
| U.S.A. (Rocky Mts.)                             | Permian                       | 298.9 to 251.9 Ma    | 30.50                           | –                             |
| Australia (Lady Annie)                          | Cambrian                      | 538.8 to 485.4 Ma    | 35.00                           | –                             |
| China   | Early Cambrian                | 538.8 to 521 Ma      | 23.41                           | –                             |
| India (Udaipur)                                 | Archean or Proterozoic        |                      | 36.46                           | –                             |
| India (Mussoorie)                               | Early Cambrian                | 538.8 to 521 Ma      | 27.22 to 32.91                  | 45.49 to 259.15               |
| India (Lalitpur)                                | Paleoproterozoic              | 2500 to 1600 Ma      | 28.78 to 31.84                  | 28.78 to 31.84                |
| Phosphorite deposits in Central Guizhou, China  | Precambrian-Cambrian boundary | 538.8 Ma             | 2.65 to 38.77                   | 10.09 to 1073.24 $\Sigma$ REY |
| Phosphorites of the Georgina Basin of Australia | Cambrian                      | 538.8 to 485.4 Ma    | 20 to 36.3                      | up to 0.5 wt% REE             |

(modified after Nathan, 1984; Cohen et al., 2013; Yang et al., 2021; Khan et al., 2012a,b; Laouar et al., 2024).

‘‘Cambrian Explosion,’’ witnessed the first main worldwide phosphogenic event, wherein the formation of phosphatic sedimentary rock (phosphorites) developed. These deposits preserve the records related to biogeochemical changes and oceanographic shifts (Papineau, 2010). This event preserved records of strontium, carbon, and oxygen isotopes, along with REE signatures found in phosphatic shallow-water deposits from regions such as Kazakhstan, Mongolia, and Queensland (Stammeier et al., 2019; Armstrong and Parnell, 2024). The ages of seafloor phosphorites range from the Cambrian to the Holocene (Table 5). In Southwest China, sedimentary phosphorites formed around the Precambrian-Cambrian transition (PC-C) exhibit significant REE enrichment, with total REE concentrations exceeding 1000  $\mu$ g/g (Xing et al., 2024). Fig. 7a shows the formation and abundance of phosphate deposits through geological time.

The absence of phosphorite in the Archean is likely due to the anoxic chemical weathering of the mafic crust that characterized the early Precambrian. This weathering would have resulted in modest dissolved phosphate, leading to an ocean with very low phosphate deposits. The lack of an oxygen-stratified ocean likely hindered phosphogenesis, as Fe-redox pumping could not operate. Without this important phosphorus shuttle, the precipitation of francolite would have been difficult, as there was no mechanism to supersaturate phosphate in pore waters (Pufahl, 2010). Phosphorite is mostly a Phanerozoic phenomenon, with a lone depositional event in the Precambrian, around 2.2 to 1.8 billion years ago, during the middle of the Great Oxidation Event, just after the Huronian Glaciation (Fig. 7b). This interval likely reflects a rise in the delivery of dissolved phosphate to the oceans, possibly due to the shift from mechanical weathering during the Huronian Glaciation to chemical weathering of continental crust under an oxygenated atmosphere. Phosphogenesis during this period appears to have been restricted to photosynthetically oxygenated, shallow-water environments, where Fe-redox pumping drove the precipitation of phosphate. Phosphorite disappeared around 1.8 billion years ago, possibly due to a decoupling of the Fe and P cycles when the sulfidic ocean environment arose. Similar to iron formations, phosphorite could not build up again until the Neoproterozoic (Pufahl, 2010).

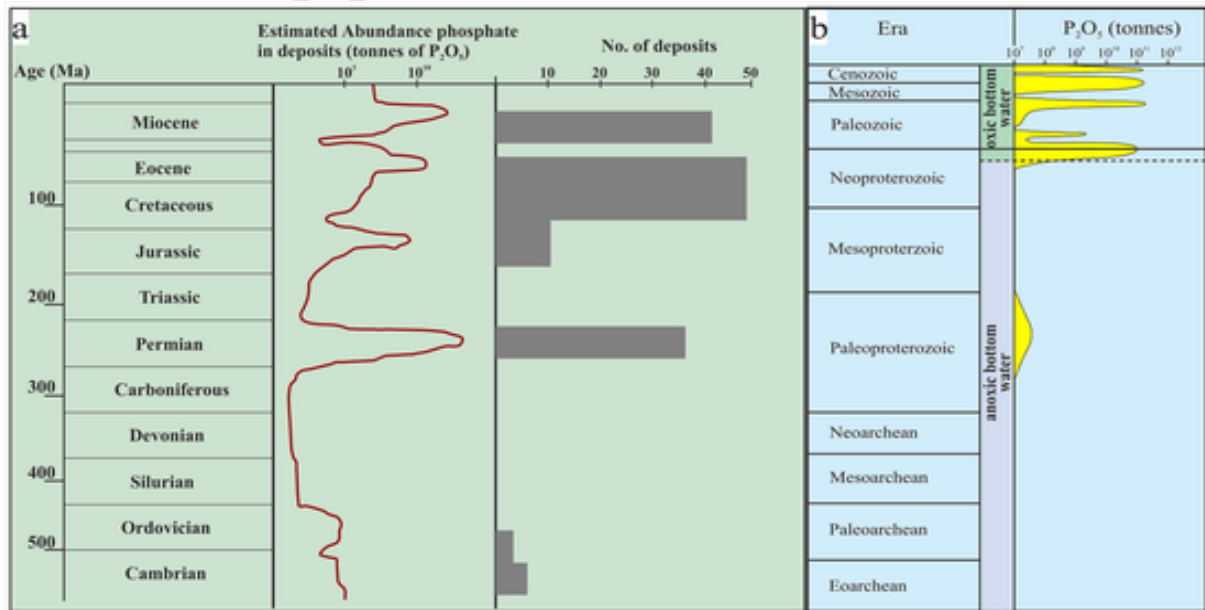


**Fig. 7.** (a) Formation and abundance of phosphate deposits through geological time (modified after Shaban, 2016), (b) Temporal distribution of phosphorite (yellow). Curves are based on deposit age and reestimates in , and (For interpretation of the references to colour in this figure legend, the reader is referred to the web version of this article.) source Glenn et al. (1994), Kholodov and Butuzova (2001) Klein (2005).

The first true giant phosphorite deposits appeared around the Neoproterozoic-Cambrian boundary (~700 to 510 million years ago) (Fig. 7b). Their deposition likely marks the permanent return of coupled Fe and P cycling in seawater after widespread sulfidic ocean conditions finally ceased. As the ocean became fully oxygenated around 580 million years ago, Fe-redox pumping could drive phosphorite formation in all shelf environments. Biological evolution during the Ediacaran and Cambrian periods also promoted phosphogenesis. The concentration of phosphorus in the biological cycle through microbial activity, fecal pellets, filter feeding, bioturbation, and the development of phosphatic shells during the Cambrian Explosion led to higher phosphorus levels in sediment (Pufahl, 2010).

During the Ordovician and Miocene, large phosphorite deposits were related to intensified coastal upwelling during glaciations (Fig. 7b). The marked equator-to-pole temperature gradient generated by high-latitude glaciers enhanced atmospheric circulation, leading to stronger coastal upwelling and extensive build-up of organic-rich sediment and phosphorite. This increase in surface ocean productivity sequestered more atmospheric carbon dioxide, driving further cooling and reinforcing the temperature gradient, which in turn strengthened coastal upwelling cells and produced even more phosphorite (Pufahl, 2010).

Phosphorite peaks during the Permian and Mesozoic also formed due to ocean-climate feedback, but were driven by warming. The green-

house climate of these periods accelerated the hydrologic cycle, increasing chemical weathering and phosphorus delivery to the oceans. Intense coastal upwelling developed along the margins of favorably positioned continents, producing large epeiric sea phosphorites (Pufahl, 2010).

Over geological time, the REE content of phosphorites has been influenced by various factors, including changes in seawater chemistry, ocean circulation, atmospheric oxygen levels, tectonic activity, and diagenetic processes. These changes reflect broader shifts in Earth's environmental conditions, making phosphorites valuable for studying past oceanic and atmospheric conditions, as well as the cycling of critical elements like phosphorus and REEs through Earth's systems.

#### 4. REEs geochemistry and their enrichment mechanism in phosphorites

The bell-shaped Rare Earth Element (REE) patterns observed in phosphorites typically reflect the diagenetic signatures of fluorapatite (Fig. 8a). Fig. 8b presents the approximate  $\Sigma$ REE concentrations in different global phosphorite deposits (modified after Haneklaus et al., 2024). Carbonate fluorapatite, the primary mineral in these deposits, exhibits varying  $P_2O_5$  concentrations across outcrops, typically ranging from 18.39 % to 30.16 % by weight. Phosphorites often display a characteristic “seawater REE pattern,” with a depletion in cerium (Ce) and

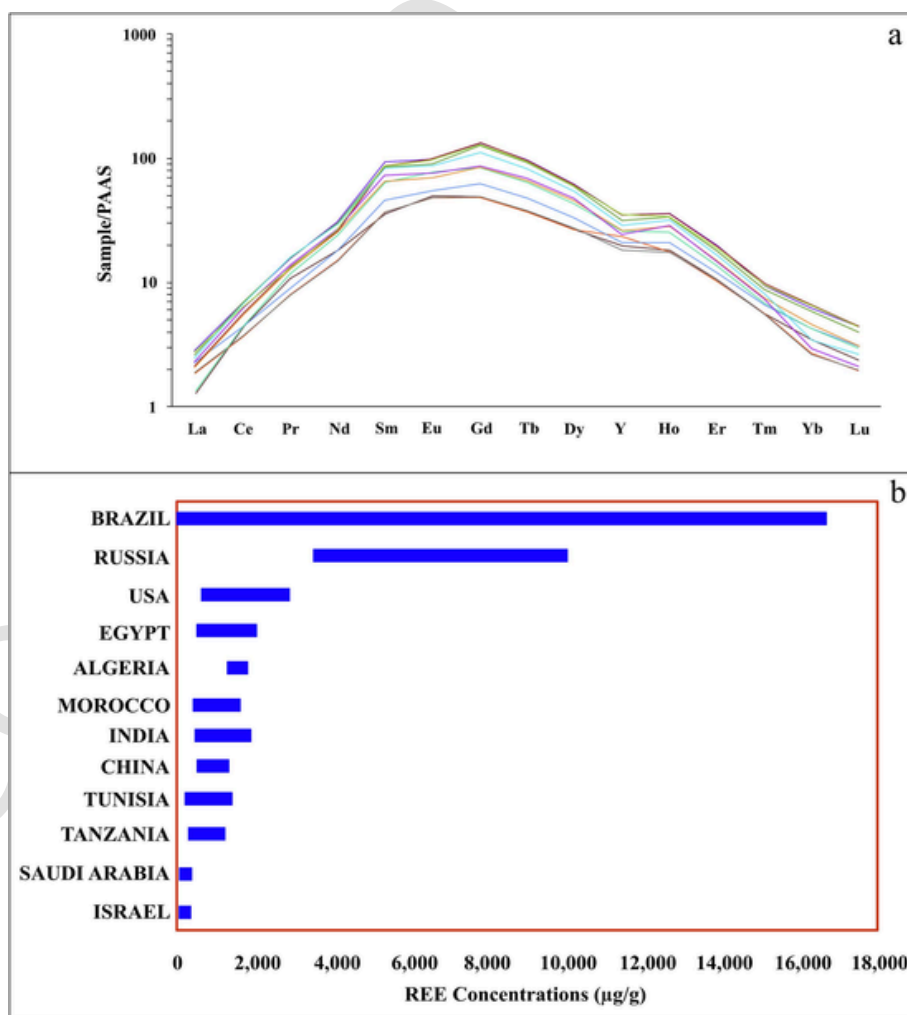


Fig. 8. (a) PAAS-normalized REE patterns phosphate nodule showing a bell shape due to the presence of high concentrations of HREE (Sasmaz et al., 2023), (b)  $\Sigma$ REE concentrations in different phosphorite deposits worldwide (modified after Haneklaus et al. (2024).

enhancement in HREE. REEs in phosphorites are valuable proxies for understanding seawater chemistry, with phosphate rock containing up to 1 % REE oxides due to isomorphous substitutions of  $\text{Ca}^{2+}$  by REE ions, particularly in minerals like REE-francolite, where REEs replace  $\text{Ca}^{2+}$  in the apatite crystal structure. Other forms of REE in phosphorites include monazite (Ce, La, Nd, Th)  $\text{P}_2\text{O}_5$ , xenotime ( $\text{YP}_2\text{O}_5$ ), allanite, and carbonates within apatite.

Studies have highlighted variable cerium (Ce) anomalies in phosphorites, with positive Ce anomalies linked to reduced conditions (Ismail, 2002; Khan et al., 2016; Dar et al., 2025). For example, phosphorites from the southwestern coast of Africa show negligible Ce anomalies, reflecting anoxic or sub-oxic conditions during their formation (Watkins et al., 1995). Similarly, europium (Eu) anomalies are observed, indicating the reduction of  $\text{Eu}^{3+}$  to  $\text{Eu}^{2+}$  under strongly reducing circumstances (Ismail, 2002). These anomalies provide insights into the redox conditions during phosphorite formation. Mazumdar et al. (1999) reported negative Ce and positive Eu anomalies in chert-phosphorite collections from the Tal Formation in India, suggesting slight oxidizing to reducing conditions. Similarly, phosphorites from the Sonrai basin in Uttar Pradesh exhibited these anomalies, further supporting the interpretation of a moderately oxidizing environment (Khan et al., 2012a, b). A PAAS-normalized REE profile by Khan et al. (2023) revealed a modest negative Ce anomaly and a positive Eu anomaly, indicative of specific diagenetic conditions. PAAS-normalized REE patterns from phosphorite samples often exhibit anomalies in Ce and Eu, reflecting redox-sensitive processes. Fig. 9 shows PAAS-normalized REE patterns from various samples, including phosphorite, francolite, dolomite, and deep-sea water from the Indian Ocean.

The redox conditions during phosphorite formation are further illuminated by the behavior of other trace elements, such as manganese (Mn), uranium (U), and vanadium (V), which are also sensitive to changes in redox conditions (Kechiched et al., 2020). These elements,

which accumulate in anoxic marine sediments, give further insight into the environment of phosphorite deposition. Phosphorites from various global deposits show significant variation in REE contents, influenced by depositional conditions, diagenetic processes, and precursor materials. REE enrichment in phosphorites arises from a combination of seawater and terrestrial inputs, along with specific redox conditions. Francolite, a form of apatite, serves as the primary host for REEs in phosphorites.

In the Zhijin phosphorite deposit, REE concentrations were primarily found in the lattice defects of apatite, with the highest concentrations in biological organisms (Xiong et al., 2024). In South China, Yang et al. (2023) confirmed that Fe/Mn (oxyhydr) oxides contribute to REE enrichment in early Cambrian phosphorites, with REEs primarily hosted in francolite. In Sri Lanka, sediments near the Eppawala Phosphate deposit contain REE-rich fluorapatite and hydroxylapatite (Dushyantha et al., 2023). In the Zhijin area of Guizhou Province, China, phosphorites exhibit Y enrichment, sourced from a combination of seawater and terrestrial inputs, rather than seafloor hydrothermal fluids (Gong et al., 2021).

Graul et al. (2023) identified multi-stage REE enhancement in shallow marine sediments, where early diagenesis and sedimentation played a crucial role in releasing REEs from Fe-(oxyhydr)oxides and organic-rich particles in anoxic circumstances. In Tunisia, high REE contents in Tertiary phosphorites correlate with the bulk porosity and surface area of cryptocrystalline apatite (Sassi et al., 2005). Similarly, Zhang et al. (2021a) suggested that the high specific surface area of francolite grains in the Zhijin deposit significantly contributed to REE enrichment. Other studies suggest that REE enrichment in phosphorites is influenced by redox circumstances in overlying seawater and the reworking of sediments (Xing et al., 2024). Wu et al. (2022) proposed that organic matter plays a key role in enriching REE in the Zhijin deposit, likely during anaerobic oxidation processes at the seawater-sediment interface.

REE enrichment is also observed in glauconite-bearing phosphorites from northeastern Algeria, where  $\Sigma\text{REE}$  concentrations exceed 1000  $\mu\text{g/g}$  (Kechiched et al., 2018). The enrichment in southern phosphorites correlates with glauconite abundance. A geochemical study of Algerian phosphorites by Laouar et al. (2024) found significant REE concentrations in the richest phosphorite sub-layer (764–2050  $\mu\text{g/g}$ ), with  $\text{P}_2\text{O}_5$  contents ranging from 19.65 to 21.32 wt%. In the Guizhou region of China, Wang and Qiao (2024) reported 30 % higher HREE contents in phosphorites, suggesting that precipitation from hydrothermal fluids in a weakly oxidized environment contributed to REE enrichment.

The relationship between  $\text{P}_2\text{O}_5$ , CaO, and F with  $\Sigma\text{REE}$  is significant in Chinese (Fig. 10) and Indian phosphorite deposits (Fig. 11), implying that apatite is the primary host for both  $\text{P}_2\text{O}_5$  and REEs in these phosphorites (modified after He et al., 2022). Hein et al. (2016) observed higher HREE concentrations in seamount phosphorites. Phosphate nodules typically contain high concentrations of REE, with apatite being the most common mineral host. These phosphorites are usually enriched in light rare earth elements (LREE), although some deep-sea and igneous phosphorites are enriched in heavy rare earth elements (HREE) (Hoshino, 2020).

## 5. Machine learning (ML) models to predict REE distribution in phosphate ore deposits

REEs, categorized as critical minerals essential for clean energy technologies, are experiencing a sharp rise in claims. However, economic deposits are found in limited geologic environments such as carbonates and ion-adsorption clays, and unconventional secondary sources, including sedimentary basins, may offer the potential to meet this requirement. Coal and its burning by-products, phosphorites, oil sands tailings, and formation waters have attracted interest for REE re-

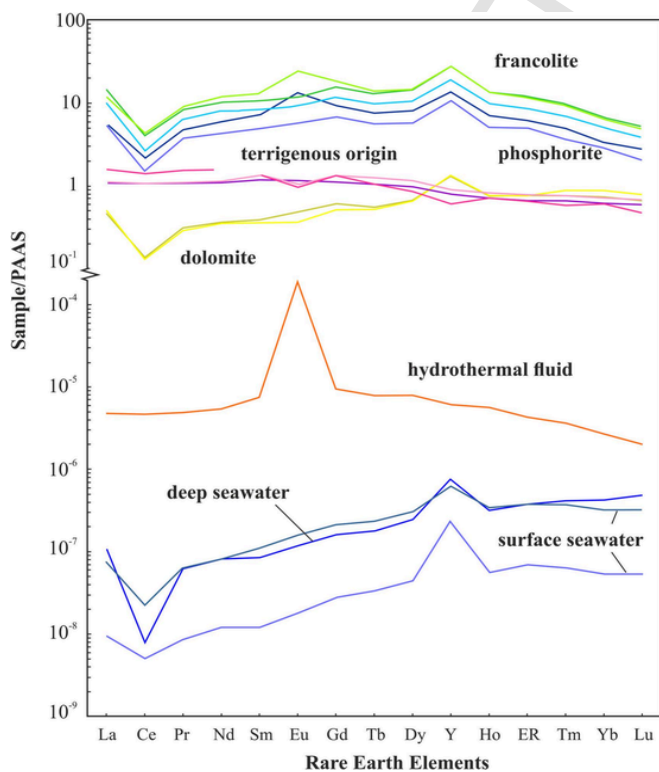
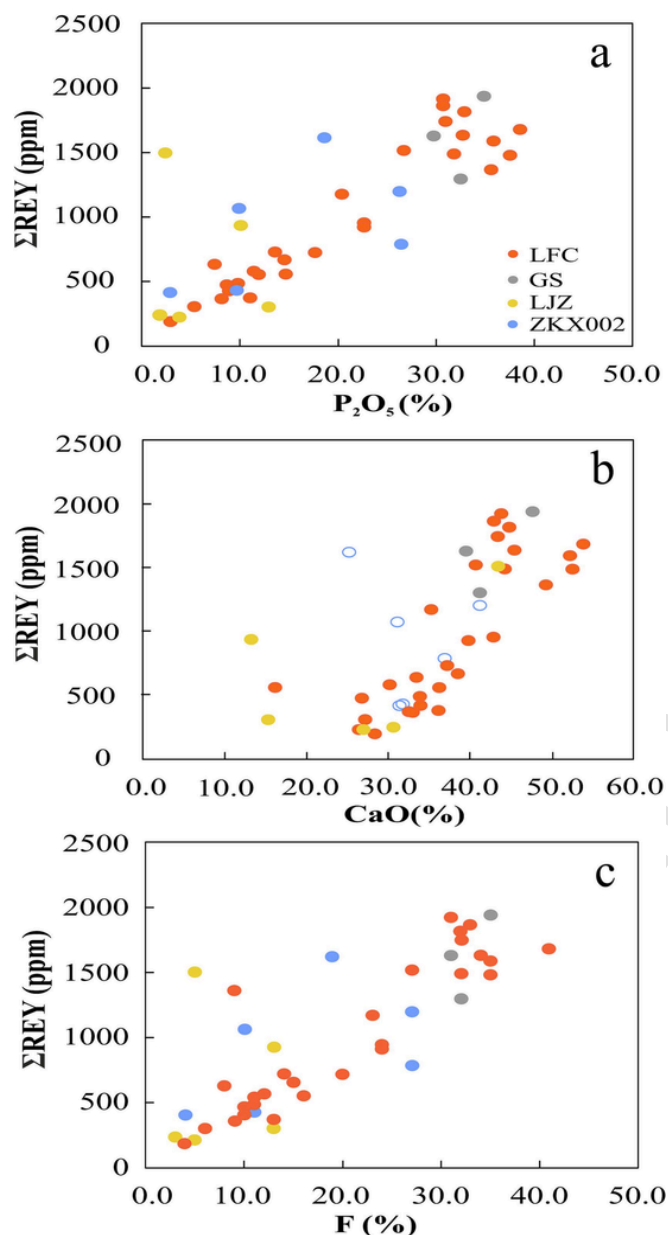


Fig. 9. PAAS-normalized REE patterns of different types of samples, including phosphorite, francolite, dolomite, and deep-sea water from the Indian Ocean (modified from He et al., 2022).



**Fig. 10.** Positive correlations between  $\Sigma\text{REY}$  and some major elements in phosphorite such as phosphorous, calcium and fluorine (a to c) with REE concentration of phosphorites from one section in Zhijin region, China (modified after He et al., 2022).

covery, though they linger largely under investigation. To address this, advanced tools like machine learning (ML) can enhance mineral prospectivity, with rapid growth in their application within Earth sciences.

The shift to a low-carbon market needs an extensive increase in metal manufacture (Lee et al., 2020), driving mineral exploration into deeper, more complex, and formerly uninvestigated areas. This expansion would demand new methods for analyzing and optimizing data throughout the exploration process, including machine-learning approaches (Cate et al., 2017). With improvements in computational power, data availability, and accessible geochemical and remote sensing datasets (e.g., Engle and Brunner, 2019; Karpatne et al., 2019), ML is increasingly applied to Earth sciences. These datasets, which typically consist of numerous samples with various variables, are well-suited for analysis by ML algorithms (Lindsay et al., 2021). ML is ap-

plied to recognize patterns in data and make predictions, with both supervised and unsupervised methods helping to understand complex relationships among variables (Cate et al., 2017). These methods are applied to forecast mineralization and elemental concentrations (Cate et al., 2017; Schnitzler et al., 2019; Grunsky and de Caritat, 2020), categorize samples (Engle and Brunner, 2019; Gregory et al., 2019), and identify patterns while reducing dimensionality (Hu et al., 2022; Lindsay et al., 2021).

The economic concentrations of REE are found in only a few geological settings (Linnen et al., 2014). Most REE production is derived from carbonatite and ion-adsorption clay deposits, which are relatively rare and, until recently, were not extensively explored (Balaram, 2019). Developing large-scale REE mining operations presents challenges and environmental concerns (Yin et al., 2021).

Machine learning has been utilized in geosciences since the 1950 s (Drams, 2020), and its uses have increased significantly presently. Modern ML techniques can handle manifold geological variables and model complex nonlinear interactions among geological factors more effectively than traditional methods (Cracknell and Reading, 2014; Li et al., 2017; Saporetti et al., 2018; Dumakor-Dupey and Arya, 2021; Zuo et al., 2021). Ore deposits of iron (Zhang et al., 2023b), copper (Esmailoghli et al., 2024), and gold (Silva Santos et al., 2022) are among the most studied using ML methods (Dumakor-Dupey and Arya, 2021). Among the broadscope of supervised ML algorithms, extreme gradient boosting (XGBoost) and random forest (RF) have emerged as some of the most effective for geochemical analysis (Parsa, 2021; Zhang et al., 2021b; Ibrahim et al., 2022, 2023; Chen et al., 2023; Ye et al., 2023; Zhang et al., 2023a, Zhang et al., 2023b). This investigation also applies decision tree (DT) and support vector regression (SVR) models.

The need for quick and reliable estimates of REE distribution in geological environments has increased. Long-established methods like inductively coupled plasma mass spectrometry are lengthy and expensive, and provide only limited point measurements, which could not capture the spatial compositional variation of a deposit. Recent research has confirmed the effectiveness of ML methods, using input variables such as  $\text{Al}_2\text{O}_3$ ,  $\text{Fe}_2\text{O}_3$ ,  $\text{TiO}_2$ , and  $\text{SiO}_2$ , to envisage the distribution of heavy REE in karst bauxite deposits in southern Italy (Buccione et al., 2023). Additionally, a freshlink between  $\text{TiO}_2$  content and the tectonic settings of Tethyan bauxite deposits was identified by applying RF and logistic regression models (Zhou et al., 2023). Machine learning models have also been used with major oxides to predict REE concentrations in ocean island basalts (Hong et al., 2019) and to forecast light REE patterns in the Choghart iron oxide-apatite deposit (Iran) (Zaremotlagh and Hezarkhani, 2017).

While industrial demand and supply conditions are crucial in defining what qualifies as an economic resource, new tools like machine learning models (ML) for data analysis can significantly enhance mineral prospectivity assessments. These ML models can predict enrichments which are also crucial for guiding future exploration programmes. Tahar-Belkacem et al. (2024) specifically developed a novel ML model to accurately predict LREE, HREE, and  $\Sigma\text{REE}$  contents in phosphorite deposits which offers cost-effective classification of the ore contents using major element concentrations. Though paleogeography, geodynamics, and depositional environment are key influencing factors, nine major element concentrations such as  $\text{SiO}_2$ , MnO,  $\text{Al}_2\text{O}_3$ , and  $\text{Fe}_2\text{O}_3$  influence the concentrations of REE as well as their patterns. Bishop and Robbins (2024) also developed ML models (correlation, principal component, and cluster analysis) to identify the different indicators of REE enrichment in sedimentary strata including phosphorite deposits. Such predictions are useful in exploration studies in addition to the cost-effective classification of phosphorite deposits. In addition, these models with certain limitations are valuable in understanding important aspects such as the local deposition environment. Paleogeography, ocean-margin tectonics, and sea-level oscillations can influence

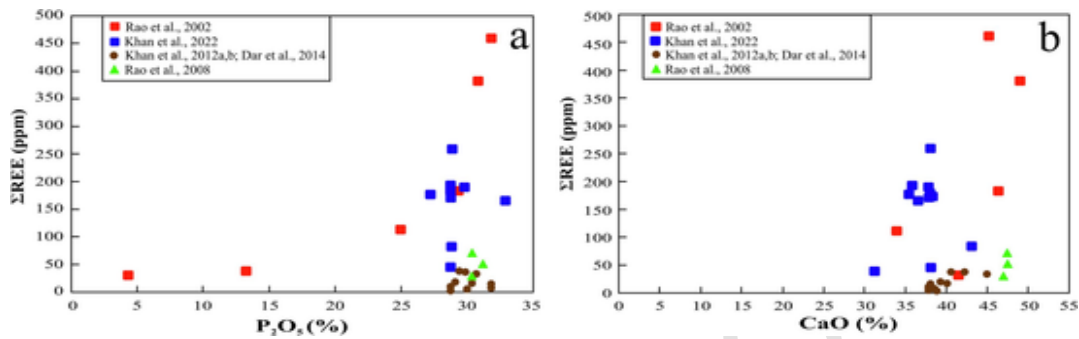


Fig. 11. Light positive correlations of phosphorous and calcium with  $\Sigma$ REE in some Indian phosphorite deposits (after Rao et al., 2002, 2008; Khan et al., 2012a, b, 2022; Dar et al., 2014).

the local depositional environments during phosphorite deposit formation.

## 6. Recovery and recycling of rare earth elements (REEs) from phosphate resources

The extraction and recuperation of REE from phosphate rock and related by-products, such as phosphogypsum, have gained increasing attention due to the rising demand for REE and their critical role in modern technologies. Extraction methods have been explored for nearly 90 years, with early research originating in the Soviet Union (Skorovarov et al., 1992; Raudsep, 2008; Jürjo et al., 2024). Phosphate rock, mainly mined from sedimentary deposits, accounts for about 80 % of global production and is typically processed to extract phosphorus as phosphoric acid.

The processing of phosphate rock generally involves sulfuric acid ( $H_2SO_4$ ) or a combination of nitric acid ( $HNO_3$ ) and hydrochloric acid (HCl) to extract REE. Leaching efficiencies as high as 80 % have been reported without interfering with fertilizer production (Habashi, 1985). REEs are typically found in minerals such as fluorapatite, dolomite, and francolite (Li et al., 2021; Emsbo et al., 2015), which can be efficiently extracted using acidic treatments. For example, studies on Chinese phosphate ores have shown that phosphoric acid can achieve leaching efficiencies for REE up to 97.8 % under optimized conditions (Li et al., 2021). Additionally, innovative methods like the use of ionic liquids (Jürjo et al., 2024) and chelating polymers (Laurino et al., 2019) have been explored for selective REE recovery.

Further advancements have been made in improving REE extraction using biological agents. Phosphate-solubilizing microorganisms, such as *Bacillus thuringiensis*, have been shown to enhance REE leaching efficiency by aiding the release of REE from resistant minerals like xenotime and monazite (He et al., 2024). The combination of acid leaching and microbial treatments has also proven effective in increasing recovery rates from phosphate ores.

Phosphogypsum ( $CaSO_4$ ), a major by-product of phosphate fertilizer production, contains a significant concentration of REE, making it an important source for their recovery (Rychkov et al., 2018; Laurino et al., 2019). The estimates suggesting that around 21 million tons of REE are currently stored in waste dumps (Yahorava et al., 2016). This number continues to grow as global phosphate production increases. The processes involved in phosphate mining and REE extraction generate waste rocks, sludge, and other by-products, which present untapped potential for REE recovery (Binnemans et al., 2015; Safhi et al., 2022).

Modern studies focus on convalescing the leaching and recovery of REE from phosphogypsum and other waste materials. For instance, Yang et al. (2019) explored various acid and organic chemical leaching methods, achieving enhanced extraction efficiencies using a two-step  $H_2SO_4$  leaching process. Additionally, advanced solvent extraction

techniques involving organic reagents like tributyl phosphine (TBP) and tri-octyl phosphine oxide (TOPO) have proven effective for extracting REE from phosphogypsum. Costis et al. (2021) demonstrated a multi-stage resin-in-leach process that achieved up to 95 % recovery of REE. Furthermore, phosphoric acid solutions, which often contain REE, can be treated with modified silica gel to prevent the accumulation of these elements in the soil (Masoud et al., 2024).

## 7. Analytical techniques

Geochemical, mineralogical, and geochronological studies are crucial for understanding the processes of REE enrichment, as well as for determining the ages of formations and the formation of phosphorite deposits across various tectonic settings and environmental conditions (Bouabdallah et al., 2019; Balaram, 2021; Balaram et al., 2022). The mineralogical composition of phosphorites is key to developing effective extraction methods for REE. For instance, a  $P_2O_5$  content greater than 20 % often indicates the dominance of apatite group minerals. Various analytical techniques are employed to gather elemental, isotopic, and mineralogical data. These include X-ray diffraction (XRD), scanning electron microscopy (SEM) with energy-dispersive X-ray spectroscopy (EDS), and laser ablation inductively coupled plasma mass spectrometry (LA-ICP-MS). For detailed textural analyses, field-emission scanning electron microscopy (FE-SEM) is used, while electron probe microanalysis (EPMA) is commonly applied to examine major, minor, and trace elements (Ferhaoui et al., 2022; Graul et al., 2023).

Fig. 12a shows SEM photomicrographs of crystalline hexagonal apatite from phosphorites in the Lalitpur district, India, captured at different resolutions. Xiong et al. (2024) utilized a range of analytical tools to investigate the mineralogy of phosphate deposits in Guizhou, China, finding that colophane and apatite were the main mineral phases. XRD analysis of phosphate rocks from the Sokoto sedimentary basin in Nigeria revealed their mineralogical composition, highlighting substantial concentrations of fluorapatite (Mustapha et al., 2022). The mineralogy of these rocks included fluorapatite, calcite, smectite, quartz, kaolinite, goethite, and palygorskite, with fluorapatite content reaching up to 79.28 %. Fig. 12b shows XRD patterns indicating the presence of carbonate-fluorapatite (CFA), quartz (Q), and feldspar (F) minerals in the Paleoproterozoic phosphorite deposits of the Bijawar Group in the Sonrai Basin, Lalitpur district, Uttar Pradesh, India.

Several studies employ techniques like ICP-MS and X-ray fluorescence spectroscopy (XRF) for elemental characterization (Graul et al., 2023; Ferhaoui et al., 2022; Balaram, 2021). Graul et al. (2024) used the in-situ imaging technique of LA-ICP-MS, alongside pathfinder elements like Sr and U, to explore the distribution and uptake mechanisms of REE within the apatite and carbonates of Estonian phosphorites, located in the Baltic paleo-basin, one of Europe's largest phosphate rock

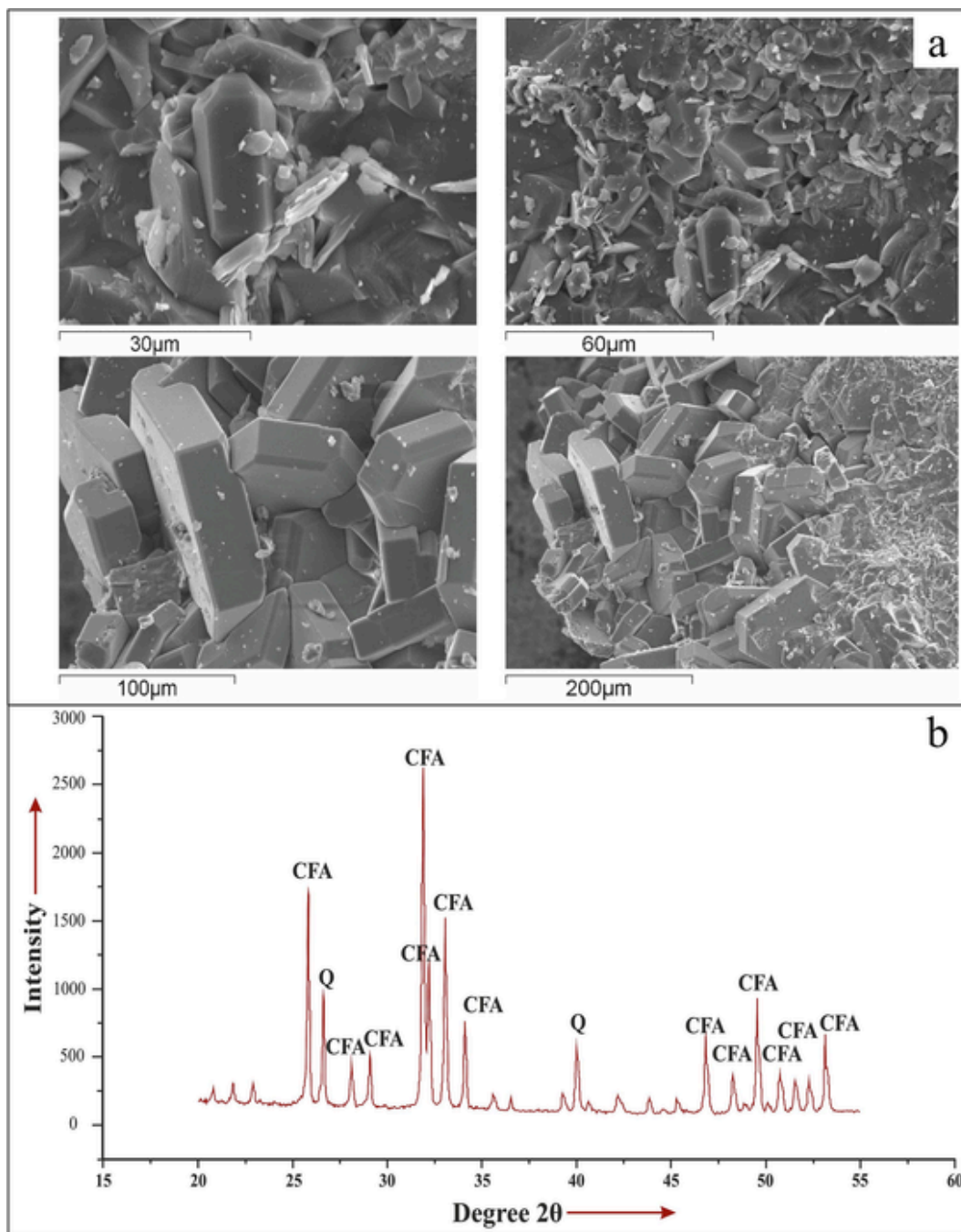


**Fig. 12.** (a) Scanning electron microscope (SEM) photomicrographs showing crystalline hexagonal apatite of Paleoproterozoic phosphorite deposits of Bijawar Group, Sonrai Basin, Lalitpur district, Uttar Pradesh, India at different resolutions (Dar et al., 2015), (b) X-ray diffraction (XRD) patterns indicating carbonate-fluorapatite (CFA), quartz (Q), and feldspar (F) minerals in Paleoproterozoic phosphorite deposits of Bijawar Group, Sonrai Basin, Lalitpur district, Uttar Pradesh, India (Dar et al., 2015).

reserves. Their findings revealed that the degree of diagenetic overprint and enrichment varied locally. Similarly, Skhurram et al. (2010) studied REE concentrations in the Kakul phosphorite deposits in Pakistan using instrumental neutron activation analysis (INAA).

Xiqiang et al. (2020) examined apatite grains from Zhijin phosphorites in China using LA-ICP-MS and EPMA, finding that REY (rare earth yttrium) entered the crystal lattice through isomorphism, rather than by inclusion in REY-bearing accessory phases. A study employing LA-ICP-MS and transmission electron microscopy (TEM) revealed that REE in the sedimentary phosphorites of Southwest China were hosted

in nanoscale francolite (Xing et al., 2024). Additionally, Sun et al. (2024) prepared a set of three CGSP-P phosphate matrix reference materials for LA-ICP-MS analysis, with certified values for elements such as Mg, Ca, P, Mn, and REE. This collaborative analytical effort involved a network of eight laboratories.

## 8. Conclusions and future

Several studies carried out in recent times demonstrate the potential of phosphorite deposits worldwide to meet a growing demand for REE

and, more importantly, that of HREE. Extraction of REE from phosphorite does not pose any major technological or environmental challenges provided the radioactive elements are removed during the extraction process. Leaching experiments show that REE can extract nearly 100 % of its total content using simple dilute  $H_2SO_4$  and HCl. In general, the strong correlation observed between phosphorus and  $\Sigma$ REE concentrations may be a helpful basis for the prediction of REE resources. REE supply from unconventional sources such as coal and its by-products, bauxite, red mud, and especially phosphorite deposits play a critical role in the future. In India, more extensive geological surveys, along with the development of new techniques and assessments, are needed to identify phosphorite deposits that contain high concentrations of REEs. These efforts would enhance the understanding of the distribution and potential of REE within phosphate deposits, which are often underexplored in the region. Improved methodologies, including advanced geochemical and mineralogical analyses, as well as cutting-edge technologies like machine learning (ML), could significantly improve the efficiency and accuracy of identifying promising REE-rich phosphorite sources. Additionally, a more thorough exploration of different tectonic settings and environments will be crucial for uncovering untapped reserves of REE within India's phosphate rock resources.

## Uncited references

Arning et al. (2009), Crosby and Bailey (2012), Dushyantha et al. (2020), Flicoteaux and Lucas (1984), Haddad et al. (2023), Hubert et al. (2005), O'Brien et al. (1981).

## CRediT authorship contribution statement

**Shamim A. Dar:** Writing – review & editing, Writing – original draft, Visualization, Validation, Software, Resources, Project administration, Methodology, Investigation, Funding acquisition, Formal analysis, Data curation, Conceptualization. **V. Balaram:** Writing – review & editing, Writing – original draft, Visualization, Validation, Supervision, Software, Resources, Project administration, Methodology, Investigation, Formal analysis, Data curation, Conceptualization. **Parijat Roy:** Supervision, Investigation, Conceptualization. **Akhtar R. Mir:** Visualization, Validation, Supervision. **Mohammad Javed:** Methodology, Formal analysis, Data curation. **M.Siva Teja:** Visualization, Validation, Supervision, Conceptualization.

## Declaration of competing interest

The authors declare that they have no known competing financial interests or personal relationships that could have appeared to influence the work reported in this paper.

## Acknowledgments

The first author pays sincere thanks to the HOD, Department of Geology, B.H.U, Varanasi for providing the necessary facilities. Shamim A. Dar is highly thankful to the Anusandhan National Research Foundation (ANRF), Science and Engineering Research Board (SERB), Department of Science & Technology, Government of India for a start-up research grant (M-14/0599; Sanction order no. SRG/2022/001478) and Seed Grant under Institutions of Eminence (IoE), Banaras Hindu University (BHU) (Dev. Scheme No. 6031) for financial assistance. Dr. V. Balaram acknowledges the support of Dr. Prakash Kumar, Director, CSIR-National Geophysical Research, Hyderabad, India.

## References

Abouzeid, A.Z.M., 2008. Physical and thermal treatment of phosphate ores-An overview. *Int. J. Mineral Proc.* 85 (4), 59–84.  
Ahmed, A.H., Aseri, A.A., Ali, K.A., 2022. Geological and geochemical evaluation of

phosphorite deposits in northwestern Saudi Arabia as a possible source of trace and rare-earth elements. *Ore Geol. Rev.* 144, 104854. <https://doi.org/10.1016/j.oregeorev.2022.104854>.

Albaum, H.G., 1952. The role of phosphorus in the metabolism of plants. In: Wolterink, L.F. (Ed.), *The Biology of Phosphorus*: East Lansing. Press, Michigan State Coll, pp. 37–75.

Alonso, E., Sherman, A.M., Wallington, T.J., Everson, M.P., Field, F.R., Roth, R., Kirchain, R.E., 2012. Evaluating rare earth element availability: a case with revolutionary demand from clean technologies. *Environ. Sci. Tech.* 46 (6), 3406–3414.

Altschuler, Z.S., Clarke, Jr, R.S., Young, E.J., 1958. Geochemistry of uranium in apatite and phosphorite. *U.S. Geol. Survey Prof. Paper* 314-D, 45–90.

Amine, M., Asafar, F., Bilali, L., Nadifyne, M., 2019. Hydrochloric Acid Leaching Study of Rare Earth Elements from Moroccan Phosphate. *J. Chem.* 2019, 675276. <https://doi.org/10.1155/2019/4675276>.

Armstrong, J., Parnell, J., 2024. Cycling of rare earth elements at the Precambrian-Cambrian boundary. *Global Planet. Change* 236, 104434. <https://doi.org/10.1016/j.gloplacha.2024.104434>.

Arning, E.T., Luckge, A., Breuer, C., Gussone, N., Birgel, D., Peckmann, J., 2009. Genesis of phosphorite crusts off Peru. *Marine Geol.* 262, 68–81.

Auer, G., Hauzenberger, C.A., Reuter, M., Piller, W.E., 2016. Orbitally paced phosphogenesis in Mediterranean shallow marine carbonates during the middle Miocene Monterey event. *Geochem. Geophys. Geosyst.* 17, 1492–1510.

Bai, Y., Zheng, S., Liu, N., Liu, Y., Wang, X., Qiu, L., Gong, A., 2024. The role of rare earths on steel and rare earth steel corrosion mechanism of research progress. *Coatings* 14, 465. <https://doi.org/10.3390/coatings14040465>.

Balaram, V., 2022. Rare earth element deposits: Sources, and Exploration Strategies. *J. Geol. Soc. India* 98, 1210–1216. <https://doi.org/10.1007/s12594-022-2154-3>.

Balaram, V., 2019. Rare earth elements: A review of applications, occurrence, exploration, analysis, recycling, and environmental impact. *Geosci. Front.* 10 (4), 1285–1303. <https://doi.org/10.1016/j.gsf.2018.12.005>.

Balaram, V., 2021. Current and emerging analytical techniques for geochemical and geochronological studies. *Geol. J.* 56 (5), 2300–2359. <https://doi.org/10.1002/gj.4005>.

Balaram, V., 2023a. Potential future alternative resources for Rare Earth Elements: Opportunities and challenges. *Minerals* 13, 425. <https://doi.org/10.3390/min13030425>.

Balaram, V., 2023b. Deep-sea mineral deposits as a source of critical metals for high-and green-technology applications. *Mineral. Mineral Mater.* 2 (5), 1–17. <https://doi.org/10.20517/mmm.2022.1>.

Balaram, V., Rahaman, W., Roy, P., 2022. Recent Advances in MC-ICP-MS Applications in the Earth, Environmental Sciences: Challenges and Solution. *Geosyst. Geoenviron.* 1, 100010. <https://doi.org/10.1016/j.geogeo.2021.100019>.

Balaram, V., Santosh, M., Satyanarayanan, M., Srinivas, N., Gupta, H., 2024. Lithium: A review of applications, occurrence, exploration, extraction, recycling, analysis, and environmental impact. *Geosci. Front.* 15, 101868.

Benitez-Nelson, C.R., 2000. The biogeochemical cycling of phosphorus in marine systems. *Earth-Sci. Rev.* 51, 109–135.

Binemans, K., Jones, P.T., Blanpain, B., Gerven, T.V., Pontikes, Y., 2015. Towards zero-waste valorisation of rare-earth-containing industrial process residues: a critical review. *J. Clean. Prod.* 99, 17e38. <https://doi.org/10.1016/j.jclepro.2015.02.089>.

Bishop, B.A., Robbins, L.J., 2024. Using machine learning to identify indicators of rare earth element enrichment in sedimentary strata with applications for metal prospectivity. *J. Geochem. Expl.* 258, 107388. <https://doi.org/10.1016/j.jexplo.2024.107388>.

Blatt, H., Tracy, R.J., 1996. *Petrology*, 2nd ed. Freeman, pp. 345–349.

Bonnot-Courtois, C., Flicoteaux, R., 1989. Distribution of rare-earth and some trace elements in Tertiary phosphorites from the Senegal Basin and their weathering products. *Chem. Geol.* 75, 311–328.

Bouabdallah, M., Elgharbi, S., Horchani-Naifer, K., Barca, D., Fattah, N., Férid, M., 2019. Chemical, mineralogical and rare earth elements distribution study of phosphorites from Sra Ouertane deposit (Tunisia). *J. Afr. Earth Sci.* 157, 1–8.

Briggs, D., Kear, A., 1993. Fossilization of soft tissue in the laboratory. *Science* 259 (5100), 1439.

Broom-Fendley, S., Siegfried, P.R., Wall, F., O'Neill, M., Brooker, R.A., Fallon, E.K., Pickles, J.R., Banks, D.A., 2021. The origin and composition of carbonate-derived carbonate-bearing fluorapatite deposits. *Mineral. Depos.* 56, 863–884.

Brouziotis, A.A., Giarra, A., Libralato, G., Pagano, G., Guida, M., Trifuoggi, M., 2022. Toxicity of rare earth elements: An overview on human health impact. *Front. Environ. Sci.* 10, 948041. <https://doi.org/10.3389/fenvs.2022.948041>.

Buccione, R., Ameer-Zaimeche, O., Ouladmansour, A., Kechiched, R., Mongelli, G., 2023. Data-centric approach for predicting critical metals distribution: heavy rare earth elements in cretaceous Mediterranean-type karst bauxite deposits, southern Italy. *Geochem. J.* 126026.

Buccione, R., Kechiched, R., Mongelli, G., Sinisi, R., 2021. REEs in the North Africa P-bearing deposits, paleoenvironments, and economic perspectives: a review. *Minerals* 11, 214. <https://doi.org/10.3390/min11020214>.

Cate, A., Perozzi, L., Gloaguen, E., Blouin, M., 2017. Machine learning as a tool for geologists. *Lead. Edge* 36, 215–219. <https://doi.org/10.1190/le36030215.1>.

Chen, Y., Li, F., Zhou, S., Zhang, X., Zhang, S., Zhang, Q., Su, Y., 2023. Bayesian optimization based random forest and extreme gradient boosting for the pavement density prediction in GPR detection. *Construct. Build Mater.* 387, 131564.

Cherepanov, A.A., Berdnikov, N.V., Shtareva, A.V., 2019. Rare-earth elements and noble metals in phosphorites of the Gremuchy Occurrence, Lesser Khingan, Far East of Russia. *Russian J. Pacific Geol.* 13 (6), 585–593. <https://doi.org/10.1134/s1819714019060022>.

Chinkaka, E., Klinger, J.M., Davis, K.F., Bianco, F., 2023. Unexpected expansion of rare-

- earth element mining activities in the Myanmar–China border region. *Remote Sens.* 15, 4597. <https://doi.org/10.3390/rs15184597>.
- Cohen, K.M., Finney, S.C., Gibbard, P.L., Fan, J.-X., 2013. The ICS International Chronostratigraphic Chart. *Episodes* 36 (3), 199–204.
- Compton, J.S., Mallinson, D., Glenn, C.R., Filippelli, G., Follmi, K.B., Shields, G., Zanin, Y., 2000. Variations in the global phosphorus cycle. In: Glenn, C.R., Prevot-Lucas, L., Lucas, J. (Eds.), *Marine authigenesis: from global to microbial*. pp. 21–33.
- Cook, P.J., Shergold, J.H., 1984. Phosphorus, phosphorites and skeletal evolution at the Precambrian-Cambrian boundary. *Nature* 308, 231–236.
- Costis, S., Mueller, K.K., Coudert, L., Neculita, C.M., Reynier, N., Blais, J.F., 2021. Recovery potential of rare earth elements from mining and industrial residues: A review and cases studies. *J. Geochem. Expl.* 221, 106699.
- Cracknell, M.J., Reading, A.M., 2014. Geological mapping using remote sensing data: a comparison of five machine learning algorithms, their response to variations in the spatial distribution of training data and the use of explicit spatial information. *Comput. Geosci.* 63, 22–33.
- Crosby, C.H., Bailey, J.V., 2012. The role of microbes in the formation of modern and ancient phosphatic mineral deposits. *Front. Microbiol.* 3, 1–7.
- Daessle, L.W., Carriquiry, J.D., 2008. Rare earth and metal geochemistry of Land and Submarine phosphorites in the Baja California Peninsula, Mexico. *Marine Georesour. Geotech.* 26, 240–349.
- Dar, S.A., 2013. Geochemical and mineralogical studies of phosphorites and associated rocks in parts of Lalitpur district, Uttar Pradesh, India. Aligarh Muslim University, Aligarh, pp. 35–54. Ph.D. thesis.
- Dar, S.A., Khan, K.F., Khan, S., Alam, M.M., 2015. Petro-mineralogical studies of the Paleoproterozoic phosphorites in the Sonrai basin, Lalitpur district, Uttar Pradesh, India. *Nat. Resour. Res.* 24 (3), 339–348.
- Dar, S.A., Khan, K.F., Khan, S.A., Mir, A.R., Wani, H., Balam, V., 2014. Uranium (U) concentration and its genetic significance in the phosphorites of the Paleoproterozoic Bijawar Group of the Lalitpur district, Uttar Pradesh, India. *Arabian J. Geosci.* 7 (6), 2237–2248. <https://doi.org/10.1007/s12517-013-0903-8>.
- Dar, S.A., Khan, K.F., Mir, A.R., Komiya, T., Absar, N., Shuaib, M., Raza, W., 2025. Geochemical and C-O isotopic study of ~2-1.9 Ga phosphate-bearing marine sedimentary rocks of the Sonrai Formation, Bijawar Group, Lalitpur district, UP, India: Implications for paleoredox, paleoclimate, and paleosalinity. *Geosyst. Geoenviron.* 4 (1), 100324.
- Deer, W.A., Howie, R.A., Zussman, J., 1962. *Rock-forming minerals, Non-silicates*. John Wiley & Sons, New York, p. 371.
- Delaney, M.L., 1998. Phosphorus accumulation in marine sediments and the oceanic phosphorus cycle. *Global Biogeochem. Cycle* 12, 563–572.
- Di, J., Ding, X., 2024. Complexation of REE in hydrothermal fluids and its significance on REE mineralization. *Minerals* 14, 531. <https://doi.org/10.3390/min14060531>.
- Dramsch, J.S., 2020. 70 years of machine learning in geoscience in review. In: Moseley, B., Krischer, L. (Eds.), *Machine learning in geosciences*. pp. 1–55.
- Drummond, J.B., Pufahl, P.K., Porto, C.G., Carvalho, M., 2015. Neoproterozoic peritidal phosphorite from the Sete Lagoas Formation (Brazil) and the Precambrian phosphorus cycle. *Sedimentology* 62, 1978–2008.
- Dumakor-Dupey, N.K., Arya, S., 2021. Machine learning—a review of applications in mineral resource estimation. *Energies* 14 (14), 4079.
- Dushyantha, D., Ratnayake, N., Premasiri, R., Batapola, B., Panagoda, H., Jayawardena, C., Chandrajith, R., Ilankoon, I.M.S.K., Rohitha, S., Ratnayake, A.S., Abeyasinghe, B., Dissanayake, K., Dilshara, P., 2023. Geochemical exploration for prospecting new rare earth elements (REEs) sources: REE potential in lake sediments around Eppawala Phosphate Deposit. Sri Lanka. *J. Asian Earth Sci.* 243, 105515. <https://doi.org/10.1016/j.jseas.2022.105515>.
- Dushyantha, N., Batapola, N., Ilankoon, I.M.S.K., Rohitha, S., Premasiri, R., Abeyasinghe, B., Ratnayake, N., Dissanayake, K., 2020. The story of rare earth elements (REEs): Occurrences, global distribution, genesis, geology, mineralogy and global production. *Ore Geol. Rev.* 122, 103521.
- Elderfield, H., Pagett, R., 1986. Analytical Chemistry in Marine Sciences Rare earth elements in ichthyoliths: variations with redox conditions and depositional environment. *Sci. Total Environ.* 49 (IS), 175–197.
- Elliott, R.B., 1973. The chemistry of gabbro/amphibolite transitions in south Norway. *Contrib. Miner. Petrol.* 38, 71–79.
- Emsbo, P., McLaughlin, P.L., Breit, G.N., du Bray, E.A., Koenig, A.E., 2015. Rare earth elements in sedimentary phosphate deposits: Solution to the global REE crisis? *Gondwana Res.* 27 (2), 776–785. <https://doi.org/10.1016/j.jgr.2014.10.008>.
- Engle, M.A., Brunner, B., 2019. Considerations in the application of machine learning to aqueous geochemistry: origin of produced waters in the Northern U.S. Gulf Coast Basin. *Appl. Comput. Geosci.* 3, 100012. <https://doi.org/10.1016/j.acags.2019.100012>.
- Esmailoghli, S., Tabatabaei, S.H., Hosseini, S., Deville, Y., Carranza, E.J.M., 2024. Blind source separation of spectrally filtered geochemical signals to recognize multi depth ore-related enrichment patterns. *Math. Geosci.* 56, 1255–1283. <https://doi.org/10.1007/s11004-023-10101-w>.
- Felitsyn, S., Morad, S., 2002. REE patterns in latest Neoproterozoic-early Cambrian phosphate concretions and associated organic matter. *Chem. Geol.* 187, 257–265.
- Ferhaoui, S., Kechiched, R., Bruguier, O., Sinisi, R., Kocsis, L., Mongelli, G., Bosch, D., Zaimche, O.A., Laouar, R., 2022. Rare earth elements plus yttrium (REY) in phosphorites from the Tébessa region (Eastern Algeria): Abundance, geochemical distribution through grain size fractions, and economic significance. *J. Geochem. Expl.* 241, 107058. <https://doi.org/10.1016/j.jgexplo.2022.107058>.
- Filippelli, G.M., 1997. Controls on phosphorus concentration and accumulation in oceanic sediments. *Mar. Geol.* 139, 231–240.
- Filippelli, G.M., 2008. The global phosphorus cycle: Past, present, and future. *Elements* 4, 89–95.
- Filippelli, G.M., 2011. Phosphate rock formation and marine phosphorus geochemistry: The deep time perspective. *Chemosphere* 84, 759–766.
- Flicoteaux, R., Lucas, J., 1984. Weathering Of Phosphate Minerals. In: Nriagu, J.O., Moore, P.B. (Eds.), *Phosphate Minerals*. Springer, Berlin, Heidelberg. 10.1007/978-3-642-61736-2\_9.
- Föllmi, K.B., 1996. The phosphorus cycle, phosphogenesis and marine phosphate-rich deposits. *Earth Sci. Rev.* 40 (1–2), 55–124.
- Garnit, H., Bouhrel, S., Barca, D., Chtara, C., 2012. Application of LA-ICP-MS to sedimentary phosphatic particles from Tunisian phosphorite deposits: insights from trace elements and REE into paleo-depositional environments. *Chem. Erde-Geochem.* 72, 127–139.
- Gerasimovsky, V.I., 1959. Geochemistry of rare earth elements. *Int. Geol. Rev.* 1 (12), 72–79.
- German, C.R., Elderfield, H., 1990. Application of the Ce anomaly as a paleoredox indicator: the ground rules. *Paleoceanography* 5, 823–833.
- German, C.R., Holliday, B.P., Elderfield, H., 1991. Redox cycling of rare earth elements in the suboxic zone of the Black Sea. *Geochim. Cosmochim. Acta* 55, 3553–3558.
- Glenn, C.R., Föllmi, K.B., Riggs, S.R., Baturin, G.N., Grimm, K.A., Trappe, J., 1994. Phosphorus and phosphorites: Sedimentology and Environments of Formation. *Eclogae Geologicae Helvetica* 87, 747–788.
- Godet, A., Föllmi, K.B., 2021. Sedimentary phosphate deposits. In: *Encyclopedia of Geology*. Elsevier, pp. 922–930. <https://doi.org/10.1016/B978-0-08-102908-4.00045-X>.
- Golroudbary, S.R., Makarava, I., Kraslawski, A., Repo, E., 2022. Global environmental cost of using rare earth elements in green energy technologies. *Sci. Total Environ.* 832, 155022. <https://doi.org/10.1016/j.scitotenv.2022.155022>.
- Gong, X., Shengwei, W., Yong, X., Zhang, Z., He, S., Xie, Z., Xiao, J., Yang, H., Tan, Q., Huang, Y., Yang, Y., 2021. Enrichment characteristics and sources of the critical metal yttrium in Zhijin rare earth-containing phosphorites, Guizhou Province, China. *Acta Geochimica* 40 (3), 441–465. <https://doi.org/10.1007/s11631-021-00460-8>.
- Gonzalez, F.J., Somoza, L., Hein, J.R., Medialdea, T., Leon, R., Urgorri, V., Reyes, J., Martin-Rubi, J.A., 2016. Phosphorites, Co-rich Mn nodules, and Fe-Mn crusts from Galicia Bank, NE Atlantic: Reflections of Cenozoic tectonics and paleoceanography. *Geochem. Geophys. Geosyst.* 17, 346–374. <https://doi.org/10.1002/2015GC005861>.
- Grandjean, P., Albarede, F., 1989. Ion probe measurement of rare earth elements in biogenic phosphates. *Geochim. Cosmochim. Acta* 53, 3179–3183.
- Grandjean-Lecuyer, P., Feist, R., Albarede, F., 1993. Rare earth elements in old biogenic apatites. *Geochim. Cosmochim. Acta* 57, 2507–2514.
- Graul, S., Kallaste, T., Pajusaar, S., Urston, K., Gregor, A., Moilanen, M., Ndiaye, M., Hints, R., 2023. REE + Y distribution in Tremadocian shelly phosphorites (Toole, Estonia): Multi-stage enrichment in shallow marine sediments during early diagenesis. *J. Geochem. Expl.* 254, 107311. <https://doi.org/10.1016/j.jgexplo.2023.107311>.
- Graul, S., Monchal, V., Rateau, R., Joosu, L., Moilanen, M., Ndiaye, M., Hints, R., 2024. LA-ICP-MS imaging technique application on Estonian sedimentary phosphorites: Revealing REE enrichment stages and advanced ore characterisation, EGU General Assembly 2024. Vienna, Austria. <https://doi.org/10.5194/egusphere-egu24-7319>.
- Gregory, D.D., Cracknell, M.J., Large, R.R., McGoldrick, P., Kuhn, S., Maslennikov, V.V., Baker, M.J., Fox, N., Belousov, I., Figueroa, M.C., Steadman, J.A., Fabris, A.J., Lyons, T.W., 2019. Distinguishing ore deposit type and barren sedimentary pyrite using laser ablation-inductively coupled plasma-mass spectrometry trace element data and statistical analysis of large data sets. *Econ. Geol.* 114, 771–786. <https://doi.org/10.5382/econgeo.4654>.
- Grunsky, E.C., de Caritat, P., 2020. State-of-the-art analysis of geochemical data for mineral exploration. *Geochem. Explor. Environ. Anal.* 20, 217–232. <https://doi.org/10.1144/geochem2019-031>.
- Habashi, F., 1985. The Recovery of the Lanthanides from Phosphate Rock. *J. Chem. Tech. Biotechnol.* 35A, 5–14. <https://doi.org/10.1002/jctb.5040350103>.
- Haddad, F., Yazdi, M., Behzadi, M., Yakymchuk, C., Khoshnoodi, K., 2023. Mineralogy, geochemistry, and depositional environment of phosphates in the Pabdeh Formation, Khormuj anticline, SW of Iran. *Environ. Earth Sci.* 82 (18), 418.
- Haley, B.A., Klinkhammer, G.P., McManus, J., 2004. Rare earth elements in pore waters of marine sediments. *Geochim. Cosmochim. Acta* 68, 1265–1279.
- Haneklaus, N.H., Mwalongo, D.A., Lisuma, J.B., Amasi, A.I., Mwimanzhi, J., Bituh, T., Ćirić, J., Nowak, J., Ryszkowski, U., Rusek, P., Maged, A., Bilal, E., Bellefqih, H., Qamouche, K., Brahim, J.A., Beniazza, R., Mazouz, H., Merwe, E.M.V.D., Truter, W., Kyomuhimbo, H.D., Waclawek, S., 2024. Rare earth elements and uranium in Minjingu phosphate fertilizer products: plant food for thought. *Resources, Conserv. Recycl.* 207, 107694. <https://doi.org/10.1016/j.resconrec.2024.107694>.
- Haxel, G.B., Hedrick, J.B., Orris, G.J., 2002. Rare earth elements critical resources for high technology. *U.S. Geological Survey, Fact Sheet* 87.
- He, S., Xia, Y., Xiao, J., Gregory, D., Xie, Z., Tan, Q., Yang, H., Guo, H., Wu, S., Gong, X., 2022. Geochemistry of REY-Enriched Phosphorites in Zhijin Region, Guizhou Province, SW China: Insight into the Origin of REY. *Minerals* 12, 408. <https://doi.org/10.3390/min12040408>.
- He, Y., Ma, L., Liang, X., Li, X., Zhu, J., He, H., 2024. Resistant rare earth phosphates as possible sources of environmental dissolved rare earth elements: Insights from experimental bio-weathering of xenotime and monazite. *Chem. Geol.* 122186. <https://doi.org/10.1016/j.chemgeo.122186>.
- Heggie, D.T., Skyring, G.W., O'Brien, G.W., Reimers, C., Herczeg, A., Moriarty, J.W., Burnett, W.C., Milnes, A.R., 1990. Organic carbon cycling and modern phosphorite formation on the east Australian continental margin: an overview. In: Notholt, A.J.G., Jarvis, I. (Eds.), *Phosphorite Research and Development*. Geol. Soc. London Special Publ., pp. 87–117.
- Hein, J.R., Koschinsky, A., Mikesell, M., Mizell, K., Glenn, C.R., Wood, R., 2016. Marine phosphorites as potential resources for heavy rare earth elements and yttrium. *Minerals* 6, 88. <https://doi.org/10.3390/min6030088>.

- Hellal, F., El-Sayed, S., Zewainy, R., Amer, A., 2019. Importance of phosphate rock application for sustaining agricultural production in Egypt. *Bull. Nat. Res. Centre* 43, 11. <https://doi.org/10.1186/s42269-019-0050-9>.
- Herwartz, D., Tutken, T., Munker, C., Jochum, K.P., Stoll, B., Sander, P.M., 2011. Timescales and mechanisms of REE and Hf uptake in fossil bones. *Geochim. Cosmochim. Acta* 75, 82–105.
- Holser, W.T., 1997. Evaluation of the application of rare-earth elements to paleoceanography. *Palaeogeogr. Palaeoclimatol. Palaeoecol.* 132, 309–323.
- Hong, J., Chengshi, G.A.N., Jie, L.I.U., 2019. Prediction of REEs in OIB by major elements based on machine learning. *Earth Sci. Front.* 26 (4), 45–54. . In Chinese with English abstract.
- Hoshino, M., 2020. Potential of apatite for heavy rare earth resource. *Chikyukagaku Geochim.* 5, 29–59. <https://doi.org/10.14934/chikyukagaku.54.29>.
- Howard, P., 1979. Phosphate. *Econ. Geol.* 74, 192–194.
- Hu, B., Zeng, L.-P., Liao, W., Wen, G., Hu, H., Li, M.Y.H., Zhao, X.-F., 2022. The origin and discrimination of high-ti magnetite in magmatic-hydrothermal systems: insight from machine learning analysis. *Econ. Geol.* 117, 1613–1627. <https://doi.org/10.5382/econgeo.4946>.
- Hubert, B., Alvaro, J.J., Chen, J.-Y., 2005. Microbially mediated phosphatization in the Neoproterozoic Doushantuo Lagerstätte, South China. *Bull. Soc. Geol. Fr.* 176, 355–361.
- Ibrahim, B., Ahenkorah, I., Ewusi, A., Majeed, F., 2023. A novel XRF-based lithological classification in the Tarkwaian paleo placer formation using SMOTE-XGBoost. *J. Geochem. Explor.* 245, 107147.
- Ibrahim, B., Majeed, F., Ewusi, A., Ahenkorah, I., 2022. Residual geochemical gold grade prediction using extreme gradient boosting. *Environ. Chall.* 6, 100421.
- Ismail, I.S., 2002. Rare earth elements in Egyptian phosphorites. *China J. Geochem.* 21, 19–28. <https://doi.org/10.1007/BF02838049>.
- Jarvis, I., Burnett, W.C., Nathan, Y., Almbaydin, F.S.M., Attia, A.K.M., Castro, L.N., Flicoteaux, R., Hilmy, M.E., Husain, V., Qutawnah, A.A., Serjani, A., Zanin, Y.N., 1994. Phosphorite geochemistry: state-of-the-art and environmental concerns. *J. Swiss Geol. Soc.* 87, 643–700.
- Jasinski, S.M., 2016. Mineral commodity summaries 2016: U.S. Geological Survey, p. 124–125, [http://minerals.usgs.gov/minerals/pubs/commodity/phosphate\\_rock/mcs-2016-phonsp.pdf](http://minerals.usgs.gov/minerals/pubs/commodity/phosphate_rock/mcs-2016-phonsp.pdf)
- Jiang, X.-D., Sun, X.-M., Chou, Y.-M., Hein, J.R., He, G.-W., Fu, Y., Li, D., Liao, J.-L., Ren, J.-B., 2020. Geochemistry and origins of carbonate fluorapatite in seamount FeMn crusts from the Pacific Ocean. *Mar. Geol.* 423, 106135.
- Jones, E.J.W., Bou Dagher-Fadel, M.K., Thirlwall, M.F., 2002. An investigation of seamount phosphorites in the Eastern Equatorial Atlantic. *Mar. Geol.* 183 (1–4), 143–162. [https://doi.org/10.1016/S0025-3227\(01\)00254-7](https://doi.org/10.1016/S0025-3227(01)00254-7).
- Jürjo, S., Oll, O., Lust, E., 2024. Yttrium separation from phosphorite extract using liquid extraction with room temperature ionic liquids followed by electrochemical reduction. *Metals* 14, 927. <https://doi.org/10.3390/met14080927>.
- Kalvoda, J., Novak, M., Babek, O., Brzobohaty, R., Hola, M., Holoubek, I., Kanicky, V., Skoda, R., 2009. Compositional changes in fish scale hydroxylapatite during early diagenesis: an example from an abandoned meander. *Biogeochemistry* 94, 197–215.
- Karpate, A., Ebert-Uphoff, I., Ravela, S., Babi, H.A., Kumar, V., 2019. Machine learning for the geosciences: challenges and opportunities. *IEEE Trans. Knowl. Data Eng.* 31, 1544–1554. <https://doi.org/10.1109/TKDE.2018.2861006>.
- Kechiched, R., Laouar, R., Bruguier, O., Salmi-Laouar, S., Kocsis, L., Bosch, D., Fougou, A., Ameur-Zaimeche, O., Larit, H., 2018. Glauconite-bearing sedimentary phosphorites from the Tébessa region (Eastern Algeria): evidence of REE Enrichment and geochemical constraints on their origin. *J. African Earth Sci.* 145, 190–200.
- Kechiched, R., Laouar, R., Bruguier, O., Kocsis, L., Laouar, S.S., Bosch, D., Zaimeche, D.A., Fougou, A., Larit, H., 2020. Comprehensive REE + Y and sensitive redox trace elements of Algerian phosphorites (Tébessa, eastern Algeria): A geochemical study and depositional environments tracking. *J. Geochem. Expl.* 208, 106396. <https://doi.org/10.1016/j.gexplo.2019.106396>.
- Khan, K.F., Dar, S.A., Khan, S.A., 2012a. Geochemistry of phosphate bearing sedimentary rocks in parts of Sonrai block, Lalitpur District, Uttar Pradesh, India. *Chemie Der Erde* 72, 117–125. <https://doi.org/10.1016/j.chemer.2012.01.003>.
- Khan, K.F., Dar, S.A., Khan, S.A., 2012b. Rare earth element (REE) geochemistry of phosphorites of the Sonrai area of Paleoproterozoic Bijawar basin, Uttar Pradesh, India. *J. Rare Earths* 30 (5), 507. [https://doi.org/10.1016/S1002-0721\(12\)60081-7](https://doi.org/10.1016/S1002-0721(12)60081-7).
- Khan, S., Dar, S.A., Khan, K.F., Shuaib, M., 2023. Rare earth element signatures of Paleoproterozoic Sallapat phosphorites of Aravalli Basin, India: implications for diagenetic effects and depositional environment. *Acta Geochim.* 42, 726–738.
- Khan, S.A., Khan, K.F., Dar, S.A., 2016. REE geochemistry of Early Cambrian phosphorites of Masrana and Kimoi blocks, Uttarakhand, India. *Arab J. Geosci.* 9, 456.
- Kholodov, V.N., Butuzova, G.Y., 2001. Problems of iron and phosphorus geochemistry in the Precambrian. *Lith. Mineral Resou.* 36, 339–352.
- Klein, C., 2005. Some Precambrian banded iron-formations (BIFs) from around the world: their age, geologic setting, mineralogy, metamorphism, geochemistry, and origin. *Am. Mineral.* 90, 1473–1499.
- Koritnig, S., 1978. Phosphorus. In: Wedepohl, K.H. (Ed.), *Handbook of Geochemistry*. Springer, Berlin, Heidelberg, New York.
- Laouar, K., Laouar, R., Bruguier, O., Bosch, D., Kechiched, D., Bouhlel, S., Tlili, A., 2024. Geochemistry of Bled El Hadba phosphorites (NE Algeria): Glauconitization process versus REE-enrichment. *J. Geochem. Expl.* 258, 107398. <https://doi.org/10.1016/j.gexplo.2024.107398>.
- Laurino, J.P., Mustacato, J., Huba, Z.J., 2019. Rare earth element recovery from acidic extracts of Florida phosphate mining materials using chelating polymer 1-octadecene polymer with 2,5-furandione, sodium salt. *Minerals* 9 (477). <https://doi.org/10.3390/min9080477>.
- Le Maitre, R.W., 2002. Igneous rocks. A classification and glossary of terms. *Recommendations of the International Union of Geological Sciences Sub-commission on the Systematics of Igneous Rocks*, second ed. Cambridge University Press, Cambridge, p. 236.
- Lecuyer, C., Reynard, B., Grandjean, P., 2004. Rare earth element evolution of Phanerozoic seawater recorded in biogenic apatites. *Chem. Geol.* 204, 63–102.
- Lee, J., Bazilian, M., Sovacool, B., Hund, K., Jowitz, S.M., Nguyen, T.P., Månberger, A., Kah, M., Greene, S., Galeazzi, C., Awuah-Offei, K., Moats, M., Tilton, J., Kukoda, S., 2020. Reviewing the material and metal security of low-carbon energy transitions. *Renew. Sust. Energ. Rev.* 124, 109789. <https://doi.org/10.1016/j.rser.2020.109789>.
- Lei, J.J., Li, R.W., Cao, J., 2000. The Characteristics of black shale hosted concretionary phosphates and the mechanisms of microbes mediated phosphorus precipitation in cambrian horizon on Yangtze platform. *Scientia Geol. Sinica* 35 (3), 277e287.
- Li, L., Solana, C., Canters, F., Kervyn, M., 2017. Testing random forest classification for identifying lava flows and mapping age groups on a single Landsat 8 image. *J. Volcanol. Geotherm.* 345, 109–124.
- Li, Z., Xie, Z., He, D., Deng, J., Zhao, H., Li, H., 2021. Simultaneous leaching of rare earth elements and phosphorus from a Chinese phosphate ore using H<sub>3</sub>PO<sub>4</sub>. *Green Proc Synt.s* 10, 258–267. <https://doi.org/10.1515/gps-2021-0023>.
- Lindsay, J.J., Hughes, H.S.R., Yeomans, C.M., Andersen, J.C.Ø., McDonald, I., 2021. A machine learning approach for regional geochemical data: Platinum-group element geochemistry vs geodynamic settings of the North Atlantic Igneous Province. *Geosci. Front.* 12, 101098. <https://doi.org/10.1016/j.gsf.2020.10.005>.
- Linnen, R.L., Samson, I.M., Williams-Jones, A.E., Chakhmouradian, A.R., 2014. Geochemistry of the rare-earth element, Nb, Ta, Hf, and Zr deposits. In: *Treatise on Geochemistry*. Elsevier, pp. 543–568. <https://doi.org/10.1016/B978-0-08-095975-7.01124-4>.
- Maallah, R., Chitaini, A., 2018. Bacterial electrode for the oxidation and detection of phenol. *Pharm Anal Acta* 9, 580. <https://doi.org/10.4172/2153-2435.1000580>.
- März, C., Riedinger, N., Sena, C., Kasten, S., 2018. Phosphorus dynamics around the sulphate-methane transition in continental margin sediments: Authigenic apatite and Fe(II) phosphates. *Marine Geol.* 404, 84–96. <https://doi.org/10.1016/j.margeo.2018.07.010>.
- Masoud, A.M., Ammar, H., Elzoghby, A.A., Agamy, H.H.E., Taha, M.H., 2024. Rare earth elements adsorption from phosphoric acid solution using dendrimer modified silica gel as well as kinetic, isotherm, and thermodynamic studies. *J. Rare Earths*. <https://doi.org/10.1016/j.jre.2024.06.012>.
- Mazumdar, A., Banerjee, D.M., Schildowski, M., Balam, V., 1999. Rare-earth elements and stable isotope geochemistry of early Cambrian chert-phosphorite assemblages from the Lower Tal formation of the Krol Belt (Lesser Himalaya, India). *Chem. Geol.* 156, 275–297. [https://doi.org/10.1016/S0009-2541\(98\)00187-9](https://doi.org/10.1016/S0009-2541(98)00187-9).
- McArthur, J.M., Walsh, J.N., 1984. Rare earth geochemistry of phosphorites. *Chem. Geol.* 47, 191–220.
- Mills, M.M., Ridame, C., Davey, M., La Roche, J., Geider, R.J., 2004. Iron and phosphorus co-limit nitrogen fixation in the eastern tropical North Atlantic. *Nature* 429, 292–294.
- Morad, S., Felitsyn, S., 2001. Identification of primary Ceanomaly signatures in fossil biogenic apatite: implication for the Cambrian oceanic anoxia and phosphogenesis. *Sediment. Geol.* 143, 259–264.
- Mustapha, S.O., Olatunji, A.S., Ajay, F.F., Isibor, R.A., 2022. Mineralogy and geochemistry of some phosphate deposits for possible rare earth elements mineralization potentials within Sokoto Basin, Northwestern Nigeria. *Indian J. Sci. Tech.* 15 (46), 2570–2578. <https://doi.org/10.17485/IJST/v15i46.1603>.
- Nash, W.P., 1984. Phosphate minerals in terrestrial igneous and metamorphic rocks. In: Nriagu, J.O., Moore, P.B. (Eds.), *Phosphate Minerals*. Springer, Berlin, Heidelberg. [https://doi.org/10.1007/978-3-642-61736-2\\_6](https://doi.org/10.1007/978-3-642-61736-2_6).
- Nathan, Y., 1984. The mineralogy and geochemistry of phosphorites. In: Nriagu, J.O., Moore, P.B. (Eds.), *Phosphate Minerals*. Springer, Berlin, Heidelberg, pp. 275–291. [https://doi.org/10.1007/978-3-642-61736-2\\_8](https://doi.org/10.1007/978-3-642-61736-2_8).
- Nelson, G.J., Pufahl, P.K., Hiatt, E.E., 2010. Paleocyanographic constraints on Precambrian phosphorite accumulation, Baraga Group, Michigan, USA. *Sediment. Geol.* 226, 9–21.
- Notholt, J.G.A., 1991. African phosphate geology and resources: A bibliography, 1979–1988. *J. Afr. Earth Sci.* 13, 543–552.
- O'Brien, G.W., Harris, J.R., Milnes, A.R., Veeh, H.H., 1981. Bacterial origin of East Australian continental margin phosphorites. *Nature* 294, 442–444.
- O'Brien, H., Heilmann, E., Heino, P., 2015. The Archaean Siilinjärvi carbonatite complex. In: Maier, W.D., Lahtinen, R., O'Brien, H. (Eds.), *Mineral Deposits of Finland*. Elsevier, pp. 327–343.
- O'Brien, G., Heggie, D., 1988. East Australian continental margin phosphorites. *EOS* 69 (1), 1–2. <https://doi.org/10.1029/88EO00007>.
- Och, L.M., Shields-Zhou, G.A., 2012. The Neoproterozoic oxygenation event: Environmental perturbations and biogeochemical cycling. *Earth-Sci. Rev.* 110, 26–57.
- Palache, C., Berman, H., Frondel, C., 1951. Dana's system of mineralogy, 7th ed. John Wiley & Sons 2, New York, p. 1124.
- Papadopoulos, A., Tzifas, I.T., Tsikos, H., 2019. The potential for REE and associated critical metals in coastal sand (placer) deposits of Greece: A review. *Minerals* 9, 469. <https://doi.org/10.3390/min9080469>.
- Papineau, D., 2010. Global biogeochemical changes at both ends of the Proterozoic: Insights from phosphorites. *Astrobiology* 10, 201. <https://doi.org/10.1089/ast.2009.0360>.
- Parker, R.J., 1971. The petrography and major element geochemistry of phosphorite nodule deposits on the Agulhas Bank, South Africa. *South Afr. Natl. Comm. Oceanogr. Res., Mar Geol. Prog. Bull. Univ. Cape Town* 2, 92–94.
- Parsa, M., 2021. A data augmentation approach to XGBoost-based mineral potential mapping: an example of carbonate-hosted ZnPb mineral systems of Western Iran. *J. Geochem. Explor.* 228, 106811.

- Paytan, A., McLaughlin, K., 2007. The oceanic phosphorus cycle. *Chem. Rev.* 107, 563–576.
- Práček, P., 2016. Phosphate rocks. <https://www.intechopen.com/chapters/49984>. In: Ptacek, P. (Ed.), *Apatites and Their Synthetic Analogues - Synthesis, Structure, Properties and Applications*. Intech Open, London. <https://doi.org/10.5772/62214>.
- Pufahl, P.K., 2010. Bioelemental sediments. In: James, N.P., Dalrymple, R.W. (Eds.), *Facies Models*. 4th ed., Geological Association of Canada, pp. 477–503.
- Pufahl, P.K., Grimm, K.A., 2003. Coated phosphate grains: proxy for physical, chemical, and ecological changes in seawater. *Geology* 31, 801–804.
- Pufahl, P.K., Groat, L.A., 2016. Sedimentary and Igneous Phosphate Deposits: Formation and Exploration: An Invited Paper. *Econ. Geol.* 112, 483–516.
- Pufahl, P.K., Hiatt, E.E., 2012. Oxygenation of the Earth's ocean atmosphere system: a review of physical and chemical sedimentological responses. *Marine Petro. Geol.* 32, 1–20.
- Rasmussen, B., 1996. Early-diagenetic REE-phosphate minerals (florentite, gorceixite, crandallite, and xenotime) in marine sandstone: a major sink for oceanic phosphorus. *J. Sci.* 296, 601–632.
- Raudsep, R., 2008. Estonian georesources in the European context. *Est. J. Earth Sci.* 57, 80.
- Reynard, B., Lecuyer, C., Grandjean, P., 1999. Crystal-chemical controls on rare-earth element concentrations in fossil biogenic apatites and implications for paleoenvironmental reconstructions. *Chem. Geol.* 155, 233–241.
- Ritterbush, S.W., 1978. Marine resources and the potential for conflict in the South China Sea. In: *Fletcher Forum of World Affairs 1983-2000*. pp. 64–85. 2(1), <http://hdl.handle.net/10427/76180>.
- Roshdy, O.E., Haggag, E.A., Masoud, A.M., Bertau, M., Haneklaus, N., Pavón, S., Hussein, A.E.M., Khawassek, Y.M., Taha, M.H., 2023. Leaching of rare earths from Abu Tartur (Egypt) phosphate rock with phosphoric acid. *J. Material Cycles Waste Manage.* 25, 501–517.
- Rychkov, V.N., Kirillov, E.V., Kirillov, S.V., Semenishchev, V.S., Bunkov, G.M., Botalov, M.S., Smyslyayev, D.V., Malyshev, A.S., 2018. Recovery of rare earth elements from phosphogypsum. *J. Clean. Prod.* 196, 674–681. <https://doi.org/10.1016/j.jclepro.2018.06.114>.
- Safhi, A.M., Amar, H., El-Berdai, Y., El-Ghorfi, M., Taha, Y., Hakkou, R., Benzaouza, M., 2022. Characterizations and potential recovery pathways of phosphate mines waste rocks. *J. Clean. Prod.* 374, 134034. <https://doi.org/10.1016/j.jclepro.2022.134034>.
- Santosh, M., Groves, D.I., Yang, C.X., 2024. Habitable planet to sustainable civilization: Global climate change with related clean energy transition reliant on declining critical metal resources. *Gondwana Res.* 1v30, 220–233. <https://doi.org/10.1016/j.jgr.2024.01.013>.
- Saporetti, C.M., da Fonseca, L.G., Pereira, E., de Oliveira, L.C., 2018. Machine learning approaches for petrographic classification of carbonate-siliciclastic rocks using well logs and textural information. *Appl. Geophys.* 155, 217–225.
- Sasmaz, A., Sasmaz, B., Soldatenko, Y., El Albani, A., Zhovinsky, E., Kryuchenko, N., 2023. Geochemical Evidence of Ediacaran Phosphate Nodules in the Volyno-Podillya-Moldavia Basin. *Ukraine. Minerals* 13, 539. <https://doi.org/10.3390/min13040539>.
- Sassi, B.A., Zaier, A., Joron, J.L., Treuil, M., 2005. Rare Earth elements distribution of tertiary phosphorites in Tunisia. *Miner. Depos. Res.* 2, 1061–1064.
- Schenau, S.J., Slomp, C.P., De Lange, G.J., 2000. Phosphogenesis and active phosphorite formation in sediments from the Arabian Sea oxygen minimum zone. *Mar. Geol.* 169, 1–20.
- Schnitzler, N., Ross, P.S., Gloaguen, E., 2019. Using machine learning to estimate a key missing geochemical variable in mining exploration: application of the random forest algorithm to multi-sensor core logging data. *J. Geochem. Explor.* 205, 106344. <https://doi.org/10.1016/j.jexplo.2019.106344>.
- Sengupta, D., Van Gosen, B., 2016. Placer-Type Rare Earth Element Deposits. *Revi. Econ. Geol.* 18, 81–100. <https://doi.org/10.1130/abs/2016AM-279551>.
- Seredin, V.V., 2010. A new method for primary evaluation of the outlook for rare earth element ores. *Geol. Ore Deposits* 52, 428–433.
- Shaban, A.M., 2016. A Review on Phosphate Deposits. Book published by American University of Beirut, p. 45.
- She, Z., Strother, P., McMahon, G., Nittler, L.R., Wand, J., Zhang, J., Sang, L., Ma, C., Papineau, D., 2013. Terminal Proterozoic cyanobacterial blooms and phosphogenesis documented by the Doushantuo granular phosphorites I: In situ microanalysis of textures and composition. *Precambrian Res.* 235, 20–35.
- Shields, G., Stille, P., 2001. Diagenetic constraints on the use of cerium anomalies as palaeoseawater redox proxies: an isotopic and REE study of Cambrian phosphorites. *Chem. Geol.* 175, 29–48.
- Sholkovitz, E.R., Landing, W.M., Lewis, B.L., 1994. Ocean particle chemistry: the fractionation of rare earth elements between suspended particles and seawater. *Geochim. Cosmochim. Acta* 58, 1567–1579.
- Silva Santos, V., Gloaguen, E., Louro, H.A.V., Blouin, M., 2022. Machine learning methods for quantifying uncertainty in prospectivity mapping of magmatic-hydrothermal gold deposits: a case study from Jurueña Mineral, Northern Mato Grosso, Brazil Province. *Minerals* 12 (8), 941. <https://doi.org/10.3390/min12080941>.
- Skhurrain, S.J., Shahida, W., Siddique, N., Shakoor, R.A., Tufail, M., 2010. Measurement of rare earth elements in Kakul phosphorite deposits of Pakistan using instrumental neutron activation analysis. *J. Radioanal. Nuclear Chem.* 284 (2), 397–403. <https://doi.org/10.1007/s10967-010-0469-9>.
- Skorovarov, J.I., Kosynkin, V.D., Moiseev, S.D., Rura, N.N., 1992. Recovery of rare earth elements from phosphorites in the USSR. *J. Alloys Compounds* 180 (1–2), 71–76.
- Slansky, M., 1986. *Geology of Sedimentary phosphates*. North Oxford Academic Publisher Ltd., Oxford, pp. 19–35.
- Slomp, C.P., Van Cappellen, P., 2007. The global marine phosphorus cycle: sensitivity to oceanic circulation. *Biogeosci.* 4, 155–171.
- Slomp, C.P., Epping, E.H.G., Helder, W., Raaphorst, W.V., 1996. A key role for iron-bound phosphorus in authigenic apatite formation in North Atlantic continental platform sediments. *J. Marine Res.* 54, 1179–1205.
- Stammer, J.A., Hippler, D., Nebel, O., Leis, A., Grengg, C., Mittermayr, F., Kasemann, S.A., Dietzel, M., 2019. Radiogenic Sr and stable C and O isotopes across Precambrian-Cambrian transition in marine carbonatic phosphorites of Malý Karatau (Kazakhstan)-Implications for paleo-environmental change. *Geochem. Geophys. Geosyst.* 20, 3–23. <https://doi.org/10.1029/2018GC007767>.
- Sun, D., Fan, C., Guo, W., Zhao, L., Zhan, X., Hu, M., 2024. Study of New CGSP-P Series Phosphate Matrix Reference Materials for LA-ICP-MS. *Geostand. Geoanal. Res.* 48 (3), 677–695.
- Tahar-Belkacem, N., Ameur-Zaimeche, Q., Kechiched, R., Ouladmansour, A., Heddam, S., Wood, D.A., Buccione, R., Mongelli, G., 2024. Machine learning models to predict rare earth elements distribution in Tethyan phosphate ore deposits: Geochemical and depositional environment implications. *Geochemistry* 84 (4), 126128. <https://doi.org/10.1016/j.chemer.2024.126128>.
- Tan, H.M.R., Huang, X.W., Qi, L., Gao, J.F., Meng, Y.M., Xie, H., 2022. Research progress on chemical composition of apatite: Application in petrogenesis, ore genesis and mineral exploration. *Acta Petrol. Sinica* 38 (10), 3067e3084.
- Taylor, S.R., McLennan, S.M., Armstrong, R.L., Tarney, J., 1981. The Composition and Evolution of the Continental Crust: Rare Earth Element Evidence from Sedimentary Rocks: Discussion. *Philosoph. Transact. B301* (1461), 398–399. <https://doi.org/10.1098/rsta.1981.0119>.
- U.S. Geological Survey. 2021. Rare Earth Statistics. In: Kelly, T.D., Matos, G.R., (Eds.), *Historical Statistics for Mineral and Material Commodities in the United States: U.S. Geological Survey Data Series 140*; US Geological Survey: Reston, Virginia, USA, 2014. Available online: <http://minerals.usgs.gov/minerals/pubs/historicalstatistics/> (accessed on 14 8 10 August 2021).
- USGS, 2024. U.S. Geological Survey, Mineral Commodity Summaries. January 2024 chrome-extension://efaidnbmnnnibpcajpcglclefindmkaj/<https://pubs.usgs.gov/periodicals/mcs2024/mcs2024-rare-earths.pdf>.
- Vadakkupuliyambatta, S., Roy, P., Ingole, B.S., Raju, K.A.K., Kurian, P.J., Meloth, T., 2024. Potential of deep-sea mineral resources for the blue economy. *Current Sci.* 126, 1–8.
- Valetich, M., Zivak, D., Spandler, C., Degeling, H., Grigorescu, M., 2022. REE enrichment of phosphorites: An example of the Cambrian Georgina Basin of Australia. *Chem. Geol.* 588, 120654. <https://doi.org/10.1016/j.chemgeo.2021.120654>.
- van der Zee, C., Slomp, C.P., van Raaphorst, W., 2002. Authigenic P formation and reactive P burial in sediments of the Nazaré canyon on the Iberian margin (NE Atlantic). *Mar. Geol.* 185, 379–392.
- Van Gosen, B.S., Verplanck, P.L., Long, K.R., Gambogi, J., Robert, R., Seal, I.I., 2014. The rare-earth elements: vital to modern technologies and lifestyles. *Fact Sheet*. 2014, 3078. <https://pubs.usgs.gov/fs/2014/3078/pdf/fs2014-3078.pdf>.
- Wang, J., Qiao, Z., 2024. Study on the material source and enrichment mechanism of REE-rich phosphorite in Zhijin. *Guizhou. Sci. Rep.* 14, 6474. <https://doi.org/10.1038/s41598-024-57074-2>.
- Wang, Z.Y., Fan, H.R., Zhou, L., Yang, K.F., She, H.D., 2020. Carbonate-Related REE Deposits: An Overview. *Minerals* 10, 965. <https://doi.org/10.3390/min10110965>.
- Warren, J.K., 2010. Evaporites though time: tectonic and eustatic controls in marine and nonmarine deposits. *Earth Sci. Rev.* 98 (3/4), 217e248.
- Watkins, R.T., Nathan, Y., Bremner, J.M., 1995. Rare earth elements in phosphorite and associated sediment from the Namibian and South African continental shelves. *Marine Geol.* 129, 111–128.
- Woolley, A.R., Kempe, D.R.C., 1989. Carbonatites: nomenclature, average chemical compositions and element distribution. In: Bell, K. (Ed.), *Carbonatites, Genesis and Evolution*. Unwin Hyman, London, pp. 1–14.
- Wright, J., Schrader, H., Holser, W.T., 1987. Paleoredox variations in ancient oceans recorded by rare earth elements in fossil apatite. *Geochim. Cosmochim. Acta* 51, 631–644.
- Wu, S., Yang, H., Fan, H., Xia, Y., Meng, Q., He, S., Gong, X., 2022. Assessment of the Effect of Organic Matter on Rare Earth Elements and Yttrium Using the Zhijin Early Cambrian Phosphorite as an Example. *Minerals* 12, 876. <https://doi.org/10.3390/min12070876>.
- Wu, C., Yuan, Z., Bai, G., 1996. Rare earth deposits in China. In: Jones, A.P., Wall, F., Williams, C.T. (Eds.), *Rare Earth Minerals—chemistry, Origin and Ore Deposits*. Chapman and Hall, New York, pp. 281–310.
- Xing, J., Jiang, Y., Xian, H., Yang, W., Yang, Y., Niu, H., He, H., Zhu, J., 2024. Rare earth element enrichment in sedimentary phosphorites formed during the Precambrian–Cambrian transition, Southwest China. *Geosci. Front.* 15, 101766. <https://doi.org/10.1016/j.gsf.2023.101766>.
- Xiong, C., Xie, H., Wang, Y., Wang, C., Li, Z., Yang, C., 2024. Microdistribution and Mode of Rare Earth Element Occurrence in the Zhijin Rare Earth Element-Bearing Phosphate Deposit, Guizhou, China. *Minerals* 14, 223. <https://doi.org/10.3390/min14030223>.
- Xiqiang, L., Hui, Z., Yong, T., Yunlong, L., 2020. REE geochemical characteristic of apatite: implications for ore genesis of the Zhijin Phosphorite. *Minerals* 10, 1012. <https://doi.org/10.3390/min1011012>.
- Yahorava, V., Bazhko, V., Freeman, M., 2016. Viability of phosphogypsum as a secondary resource of rare earth elements. In: *IMPC 2016: XXVIII International Mineral Processing Congress Proceedings at Quebec*. ISBN: 978-1-926872-29-2.
- Yang, H.Y., Xiao, J.F., Hu, R.Z., Xia, Y., He, H.X., 2020. Formation environment and metallogenic mechanism of weng'an phosphorite in the early sinian. *J. Palaeogeog.* 22 (5), 929e946.
- Yang, H., Xiao, J., Xia, Y., Xie, Z., Tan, Q., Xu, J., He, S., Wu, S., Liu, X., Gong, X., 2021. Phosphorite generative processes around the Precambrian-Cambrian boundary in South China: An integrated study of Mo and phosphate O isotopic compositions. *Geosci. Front.* 12, 101187. <https://doi.org/10.1016/j.gsf.2021.101187>.

- Yang, H.Y., Zhao, Z.F., Fan, H.F., Zeng, M., Xiao, J.F., Liu, X.Q., Wu, S.W., Chao, J.Q., Xia, Y., 2023. Fe-(oxyhydr)oxide participation in REE enrichment in early Cambrian phosphorites from South China: Evidence from in-situ geochemical analysis. *J. Asian Earth Sci.* 259, 105910. <https://doi.org/10.1016/j.jseae.2023.105910>.
- Yang, X.S., Salvador, D., Makkonen, H.T., Pakkanen, L., 2019. Phosphogypsum Processing for Rare Earths Recovery-A Review. *Nat. Resour.* 10, 325–336. <https://doi.org/10.4236/nr.2019.109021>.
- Ye, M., Zhu, L., Li, X., Ke, Y., Huang, Y., Chen, B., Yu, H., Li, H., Feng, H., 2023. Estimation of the soil arsenic concentration using a geographically weighted XGBoost model based on hyperspectral data. *Sci. Total Environ.* 858, 159798.
- Yerkebulan, R., Perizat, A., Ulzhalgas, N., 2023. Enrichment of low-grade phosphorites by the selective leaching method. *Green Proc. Synth.* 12 (1), 20228150. <https://doi.org/10.1515/gps-2022-8150>.
- Yin, X., Martineau, C., Demers, I., Basiliko, N., Fenton, N.J., 2021. The potential environmental risks associated with the development of rare earth element production in Canada. *Environ. Rev.* 29, 354–377. <https://doi.org/10.1139/er-2020-0115>.
- Young, R.A., 1975. Some aspects of crystal structural modeling of biological apatites. In: *Physico-Chimie et Cristallographie Des Apatites D'interet Biologique*. C. N. R. S, Paris, pp. 21–40.
- Yuan, W., Liu, G.D., Luo, W.B., Li, C.Z., Xu, L.M., Niu, X.B., Ai, J.Y., 2016. Species and formation mechanism of apatites in the 7(th) member of Yanchang Formation organic-rich shale of Ordos Basin. *China. Nat. Gas Geosci.* 27 (8), 1399e1408.
- Yu, L.M., Liu, M.X., Dan, Y., Said, N., Wu, J.-H., Ming-Cai, H., Zou, H., 2023. The origin of Ediacaran phosphogenesis event: New insights from Doushantuo Formation in the Danzhai phosphorite deposit. *South China. Ore Geol. Rev.* 152, 105230.
- Zanin, Yu.N., Zamirailova, A.G., 2007. Trace elements in supergene phosphorites. *Geochem. Int.* 45 (8), 758–769.
- Zaremotlagh, S., Hezarkhani, A., 2017. The use of decision tree induction and artificial neural networks for recognizing the geochemical distribution patterns of LREE in the Choghart deposit. *Central Iran. J. African Earth Sci.* 128, 37–46.
- Zhang, B., Li, M., Li, W., Jiang, Z., Khan, U., Wang, L., Wang, F., 2021a. Machine learning strategies for lithostratigraphic classification based on geochemical sampling data: a case study in area of Chahanwusu River, Qinghai Province. *China. J. Cent. South Univ.* 28, 1422–1447.
- Zhang, P., Zhang, Z., Yang, J., Cheng, Q., 2023a. Machine learning prediction of ore deposit genetic type using magnetite geochemistry. *Nat. Resour. Res.* 32 (1), 99–116.
- Zhang, W., He, Y., Wang, L., Liu, S., Meng, X., 2023b. Landslide susceptibility mapping using random forest and extreme gradient boosting: A case study of Fengjie. *Chongqing. Geol. J.* 58.
- Zhang, Z., Jiang, Y., Niu, H., Xing, J., Yan, S., Weng, Q., Zao, X., 2021b. Enrichment of rare earth elements in the early Cambrian Zhijin phosphorite deposit, SW China: Evidence from francolite micro-petrography and geochemistry. *Ore Geol. Rev.* 138, 104342. <https://doi.org/10.1016/j.oregeorev.2021.104342>.
- Zhou, J., Yu, W., Wei, W., Yang, M., Du, Y., 2023. Provenance and tectonic evolution of bauxite deposits in the tethys: perspective from random forest and logistic regression analyses. *Geochem. Geophys. Geosyst.* 24, e2022GC010745.
- Zuo, R., Wang, J., Xiong, Y., Wang, Z., 2021. The processing methods of geochemical exploration data: past, present, and future. *Appl. Geochem.* 132, 105072.



**Shamim A. Dar** is currently working as an Assistant professor, at the Department of Geology, Banaras Hindu University (BHU), Varanasi, India. He did his Ph.D from Aligarh Muslim University, Aligarh, India, and his M.Sc and B.Sc from the University of Kashmir, Srinagar, J & K, India. Before, joining BHU, he worked as a lecturer in the higher education department of J & K for more than 05 years. He has published 20 papers in SCI international and national journals and 02 book chapters. He is also a member of the governing council of the journal Indian Association of Sedimentologists. His area of specialization is sedimentary geochemistry, stable isotope geochemistry, economic geology, geoheritage, geotourism and geoparks. Presently he is guiding 06 Ph.D students and one postdoc in different fields of geology, fostering future leaders in geoscience.



**V. Balaram** is a Former Emeritus Scientist at the Geochemistry Division, CSIR - National Geophysical Research Institute, Hyderabad, India. He authored over 340 SCI publications, which were cited ~ 9,300 times (*h-index 48, i-10 index 156*), and guided 5 Ph.D. students. He has received several prestigious national and international awards such as the “**National Geoscience Award**” **Top 2% of Scientists in the World**” from the Government of India, New Delhi (2000), included in Stanford University's list of the “*in 2020, 2021, 2022, 2023 & 2024*”, “**The Academician Sazhin Medal 2024**” “**GSF Highly Cited Paper Award 2024**” from Russia, and the for his 2019 publication on REE from the *Geoscience Frontiers* (Elsevier).



**Parijat Roy** is a senior scientist at National Centre for Polar and Ocean Research, Ministry of Earth Sciences. His research area is mainly focused in deep sea mineral exploration and in understanding the complex behaviour of metals in hydrothermal circulation process in MORB's. He is also involved in developing analytical protocols for the accurate determinations of metals in various types of geological samples.



**Akhtar R. Mir** serves as an Assistant Professor in the Department of Earth Sciences at the University of Kashmir, India, where he is making significant contributions to the field of Geology. He has published around 25 research papers in reputed journals. His research interests encompass petrology, geochemistry, and tectonics. In 2018, he was honoured with the prestigious “*Smt. Ketharaju Venkata Subbamma-Sri. Subba Rao Medal*” by the Indian Society of Applied Geochemists (ISAG) for his contributions to geochemistry applied to mineral resources. He has carried out geological fieldworks in Orisha, Ladakh, Kashmir, and Rajasthan. An inspiring mentor, he has guided numerous M.Sc. Geology students through both major and minor projects, nurturing the next generation of geoscientists.



**Mohammad Javed** is a research scholar (Ph.D. student) working under the supervision of Dr. Shamim Ahmad Dar at the Department of Geology, Banaras Hindu University,

Varanasi, India. He has completed his Master's and Bachelor's degrees from the Department of Geology, Aligarh Muslim University, Aligarh, India. He has qualified CSIR-UGC JRF (AIR-21) in 2024, CSIR-NET in 2023, and also qualified GATE (2023, 2024) exami-

nations. His research interests include sedimentary geochemistry, and economic ore deposits.

CORRECTED PROOF